iScience

CellPress

Article

Biocomputational Analyses and Experimental Validation Identify the Regulon Controlled by the Redox-Responsive Transcription Factor RpaB

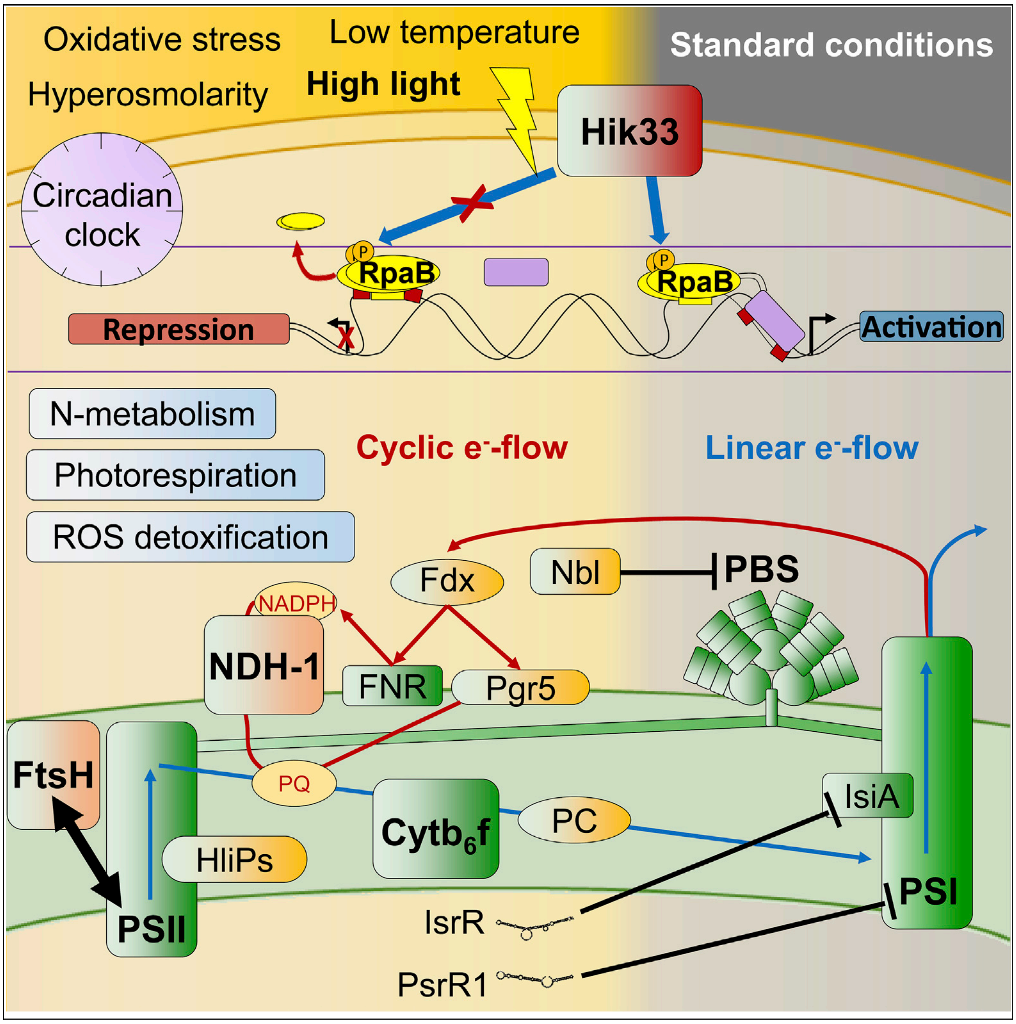

Matthias Riediger, Taro Kadowaki, Ryuta Nagayama, Jens Georg, Yukako Hihara, Wolfgang R. Hess

hihara@mail.saitama-u.ac.jp (Y.H.)
wolfgang.hess@biologie.uni-freiburg.de (W.R.H.)

HIGHLIGHTS

RpaB controls a complex regulon, widely beyond the photosynthetic machinery

The expression of the RNA regulators IsrR, PsrR1, and others depends on RpaB

RpaB exhibits cross-regulations with other transcription factors, NtcA and Fur

RpaB is a crucial transcriptional regulator in a photosynthetic microorganism

Riediger et al., iScience *15*, 316–331
May 31, 2019
https://doi.org/10.1016/j.isci.2019.04.033

iScience

CellPress

Article

Biocomputational Analyses and Experimental Validation Identify the Regulon Controlled by the Redox-Responsive Transcription Factor RpaB

Matthias Riediger,[1,4] Taro Kadowaki,[2,4] Ryuta Nagayama,[2] Jens Georg,[1] Yukako Hihara,[2,*] and Wolfgang R. Hess[1,3,5,*]

SUMMARY

Oxygenic photosynthesis requires the coordination of environmental stimuli with the regulation of transcription. The transcription factor RpaB is conserved from the simplest unicellular cyanobacteria to complex eukaryotic algae, representing more than 1 billion years of evolution. To predict the RpaB-controlled regulon in the cyanobacterium *Synechocystis*, we analyzed the positional distribution of binding sites together with high-resolution mapping data of transcriptional start sites (TSSs). We describe more than 150 target promoters whose activity responds to fluctuating light conditions. Binding sites close to the TSS mediate repression, whereas sites centered ~50 nt upstream mediate activation. Using complementary experimental approaches, we found that RpaB controls genes involved in photoprotection, cyclic electron flow and state transitions, photorespiration, and *nirA* and *isiA* for which we suggest cross-regulation with the transcription factors NtcA or FurA. The deep integration of RpaB with diverse photosynthetic gene functions makes it one of the most important and versatile transcriptional regulators.

INTRODUCTION

RpaB (''regulator of phycobilisome association B'') is an OmpR-type transcription factor of crucial importance for the transcriptional control of multiple photosynthesis-associated genes under varying light conditions. RpaB was discovered in the cyanobacterium *Synechocystis* sp. PCC 6803 (from here *Synechocystis* 6803) based on its ability to affect the energy distribution from phycobilisomes (PBS) to photosystem I (PSI) relative to photosystem II (PSII) (Ashby and Mullineaux, 1999). Orthologs of *rpaB* belong to the cyanobacterial core genome and were discovered in the chloroplast genomes of all non-green algae except *Odontella* (Martin et al., 2002) and in the charophyte alga *Chlorokybus atmophyticus* (Riediger et al., 2018), suggesting important and evolutionarily widely conserved functions. The *rpaB* gene cannot be deleted by conventional methods, indicating its essentiality (Ashby and Mullineaux, 1999; Kappell et al., 2006; Kato et al., 2011; López-Redondo et al., 2010; van Waasbergen et al., 2002). Despite its wide distribution, most insight into the genes controlled by RpaB have been obtained from analyses in two model cyanobacteria, *Synechocystis* 6803 and *Synechococcus elongatus* PCC 7942 (from here *S. elongatus*).

The RpaB-binding motif consists of a pair of imperfect 8-nt long direct repeats (G/T)TTACA(T/A) (T/A) separated by two random nucleotides. This motif was found upstream of many genes responding to high light (HL) in both *Synechocystis* 6803 and *S. elongatus* and was named the HLR1 (''high light regulatory 1'') sequence (Eriksson et al., 2000; Kappell et al., 2006). The binding of RpaB to the HLR1 sequence was first demonstrated for the *hliB* gene promoter in *Synechocystis* 6803 (Kappell and van Waasbergen, 2007). Binding to HLR1 promoter elements of the *hliA* and *hliB* genes encoding HL-inducible proteins leads to repression under low light (LL), both in *Synechocystis* 6803 and *S. elongatus* (Kappell and van Waasbergen, 2007; López-Redondo et al., 2010; Seki et al., 2007). Chromatin immunoprecipitation (ChIP) analysis showed that the binding activity of RpaB to the *hliA* and *rpoD3* promoters in *S. elongatus* was promptly lost upon a shift to HL (Hanaoka and Tanaka, 2008), leading to de-repression of these HL-inducible genes. The same mode of transcriptional regulation was reported for the small RNA (sRNA) gene *psrR1* in *Synechocystis* 6803 (Kadowaki et al., 2016). For several genes encoding PSI proteins, binding of RpaB to HLR1 was identified to be crucial for the transcription activation under LL (Seino et al., 2009; Takahashi et al., 2010). Chromatin affinity purification (ChAP) analysis revealed that loss of binding activity of RpaB upon the shift to HL leads

[1]Genetics & Experimental Bioinformatics, Institute of Biology III, Faculty of Biology, University of Freiburg, Schänzlestr. 1, 79104 Freiburg, Germany

[2]Graduate School of Science and Engineering, Saitama University, Saitama 338-8570, Japan

[3]Freiburg Institute for Advanced Studies, University of Freiburg, Albertstr. 19, 79104 Freiburg, Germany

[4]These authors contributed equally

[5]Lead Contact

*Correspondence: hihara@mail.saitama-u.ac.jp (Y.H.), wolfgang.hess@biologie.uni-freiburg.de (W.R.H.)

https://doi.org/10.1016/j.isci.2019.04.033

to a large decline in the transcript levels of PSI genes, whereas the expression of PsrR1 is induced (Kadowaki et al., 2016). PsrR1 is a negative post-transcriptional regulator of genes encoding phycobiliproteins and subunits of PSI (Georg et al., 2014), leading to the dual repression of PSI genes under HL, at the transcriptional level by RpaB and at the post-transcriptional level by PsrR1 (Kadowaki et al., 2016). The effect of RpaB binding on target promoters, which may be activation or repression under LL, is likely determined by the location of the HLR1 motif. However, some of the mentioned genes underlie complex transcriptional controls, including multiple transcriptional start sites (TSSs) belonging to separate promoters. This is the case for the *psaAB* dicistron, for which three separate TSSs and three distinct HLR1 elements have been detected in *Synechocystis* 6803. Of these, two activate and one represses transcription under LL, and it is the joint regulation at these three sites that leads to the observed regulation (Takahashi et al., 2010). In *S. elongatus*, in addition to photosynthesis-related genes, RpaB binds to the promoters of the sigma factor genes *rpoD3* and *rpoD6*, and also the promoter of the core circadian clock genes *kaiBC* (Espinosa et al., 2015; Hanaoka et al., 2012). To date, 83 occurrences of the HLR1 motif have been reported, including examples from several different cyanobacteria, the *Cyanophora* chloroplast, and cyanophage genomes (Riediger et al., 2018).

Therefore it is established that the regulon controlled by RpaB consists of genes encoding photosynthesis-related proteins as well as at least one sRNA and that this regulation is of crucial importance in light acclimation responses and circadian clock-related processes (Piechura et al., 2017). In contrast, its cognate histidine kinase Hik33 (synonyms NblS or DspA) functions as multistress sensor responding not only to HL (Tu et al., 2004) but also to low temperature (Suzuki et al., 2000), hyperosmolarity (Mikami et al., 2002), high salinity (Marin et al., 2003), oxidative stress (Kanesaki et al., 2007), and nutrient stress (van Waasbergen et al., 2002). Therefore it is likely that only a small portion of the RpaB functions has been discovered thus far. In particular, a global definition of the RpaB regulon is missing.

Here, we combined existing data from the genome-wide high-precision mapping of TSSs (Kopf and Hess, 2015; Kopf et al., 2014; Mitschke et al., 2011) with the precise identification of regulated promoters, *in silico* motif prediction, functional enrichment analysis, and validation experiments to infer the RpaB regulon in a comprehensive way, choosing *Synechocystis* 6803 as a model.

RESULTS

HLR1 Elements Are Predicted at Two Distinct Positions Relative to the TSS

Based on the sequence alignment of 90 previously reported HLR1 motifs associated with 83 promoters in *Synechocystis* 6803, *S. elongatus*, other cyanobacteria, and eukaryotic algae (Riediger et al., 2018), a position-specific weight matrix (PSWM) was generated (Figure S1), which served as input for the global motif search, as outlined in Figure 1. We analyzed the positional distribution of 3,615 theoretically possible HLR1 sites (Table S1) in the promoters of 1,992 transcriptional units (TUs) in *Synechocystis* 6803. HLR1 elements clustered at two distinct sites, centered ~51 nt upstream of the TSS or overlapping the TSS (centered at position −5) (Figure 2A). The precise positions for these two enriched HLR1 occurrences were centered in a range from −66 nt to −45 nt and from −38 nt to +23 nt relative to the respective TSS and correspond to the HLR1 center. By comparing the respective promoters against comparative primary transcriptome data (Kopf et al., 2014), these two distinct peaks matched different expression profiles. Genes with an HLR1 at or close to the TSS were generally more upregulated under HL, whereas genes with an HLR1 at −51 were generally more downregulated under HL (Figure S2). Therefore the peak around −51 was identified as belonging to HL-repressed/LL-activated promoters, whereas the motifs centered at −5 belong to HL-activated/LL-repressed promoters (Figure 2B). This is consistent with previous reports showing that binding of RpaB to HLR1 more distally located to the TSS is crucial for activating transcription under LL (Seino et al., 2009; Takahashi et al., 2010), whereas de-repression under HL, e.g., of PsrR1, was connected to an HLR1 motif overlapping the TSS (Kadowaki et al., 2016). However, here this observation is extended to a large set of promoters. Hence, depending on the distance between the HLR1 sequence and the TSS, RpaB can be either stimulating or repressing (see also Riediger et al., 2018; Wilde and Hihara, 2016 for review). For clarity, we will speak of genes activated or repressed by RpaB under LL when referring to these regulatory phenomena in the remainder of the article.

The relative location of the binding motif is likely strongly connected to the mechanism of activation, for which the cyclic AMP-Crp activator complex in *E. coli* is probably the best understood example (Lawson

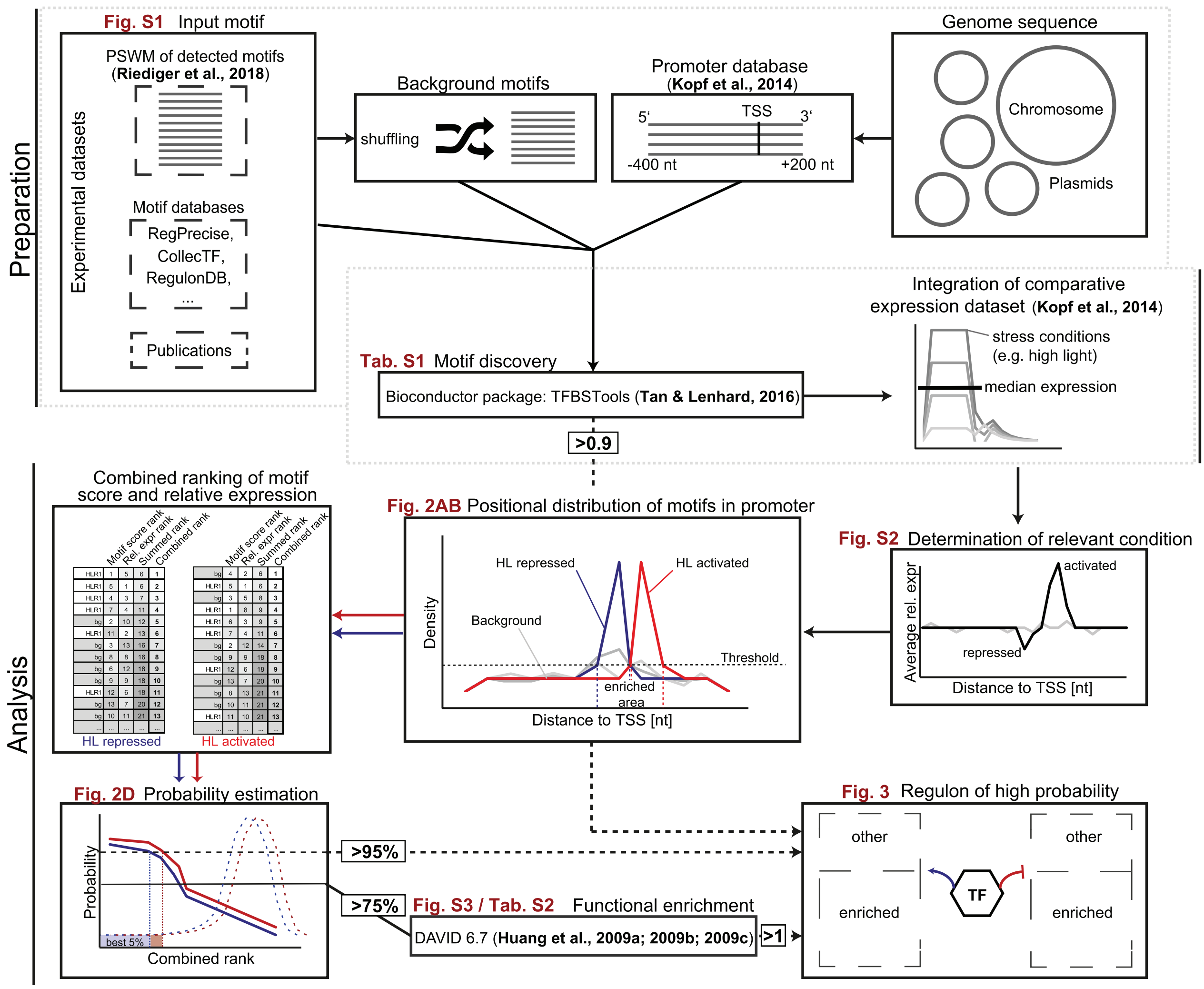

Figure 1. Bioinformatic Workflow: Preparation

A *Synechocystis* 6803 promoter database was created by extracting sequences from −400 nt to +200 nt relative to the transcriptional start sites (TSSs) of all transcriptional units (TUs) in 5′ to 3′ orientation as identified previously (Kopf et al., 2014). The HLR1 input motif was defined as a position-specific weight matrix (PSWM, Figure S1) via the alignment of all published HLR1 sequences (Riediger et al., 2018). The background motifs were generated by permuting the columns of the PSWM. Data collection: Motif detection was performed using the Bioconductor TFBSTools package (Tan and Lenhard, 2016). The comparative dRNA-seq gene expression dataset by Kopf et al. (2014) was integrated with the results, and the relative expression under each of the 10 tested conditions was normalized against the median expression of the gene of interest (Table S1). Analysis: The average relative expression level of each promoter with an HLR1 was plotted against the relative distance to the TSS to determine conditions correlating with a particular location. High light (HL) was identified as a relevant condition for further analysis (Figure S2). Subsequently, the positional distribution of the HLR1 within the promoters was examined (Figure 2A). Motifs whose promoters were activated or repressed under the relevant condition were separated before this analysis, and the density of detected motifs in activated or repressed promoters was plotted against their relative distance to the TSS (Figure 2B). Areas exceeding a density threshold of ≥99% were considered significantly enriched, and only motifs occurring in one of these areas were used for further analysis. Motifs from each enriched area were ranked according to their motif score and relative expression, and probabilities were calculated from the overall distribution of the motifs' combined ranks (Figure 2D). A probability threshold of ≥75% was set to perform a functional enrichment analysis of all genes meeting this criterion (Figure S3, Table S2) by using DAVID 6.7 (Huang et al., 2009a, 2009b, 2009c). All genes in a group with an enrichment score ≥1, a probability ≥95%, or a relative motif score ≥0.90 were accepted for the final regulon (Figure 3). The regulon was visualized using Cytoscape 3.5.1 (Cline et al., 2007).

et al., 2004). Crp facilitates upon DNA binding the recruitment of RNA polymerase (RNAP) to the promoter to yield the RNAP-promoter closed complex, and in case of the class II promoters, also the formation of the RNAP-promoter open complex (Lawson et al., 2004). Such interactions with the C-terminal domain of the RNAP α subunit are conceivable for RpaB as well.

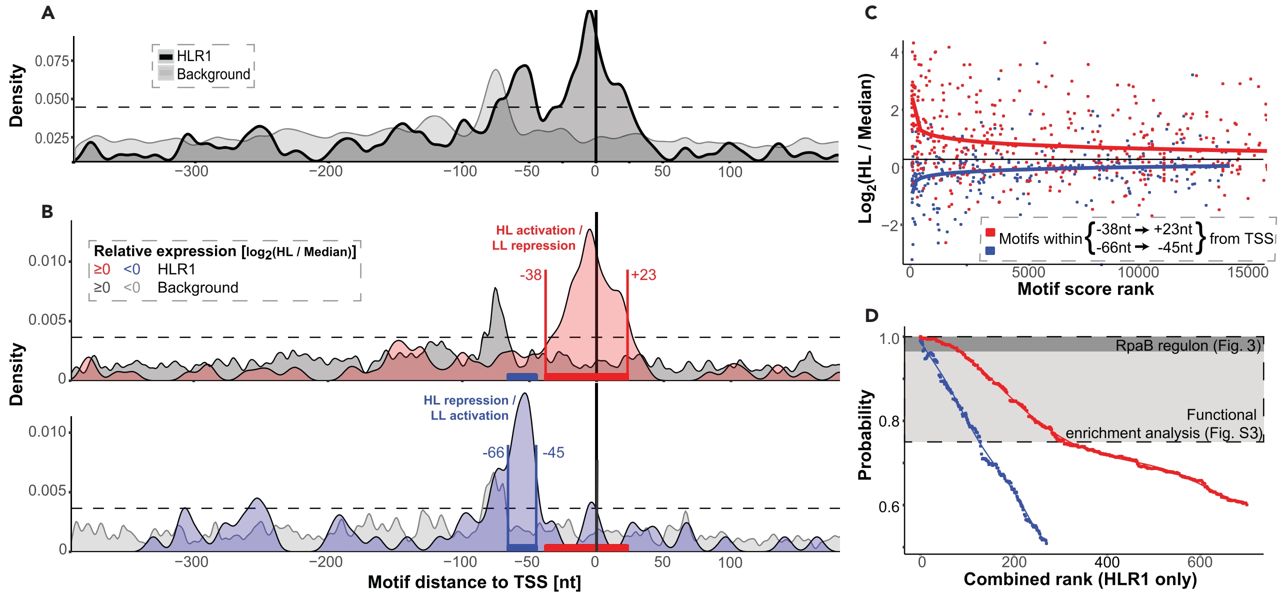

Figure 2. Bioinformatic Analysis of HLR1 Occurrences in *Synechocystis* 6803

(A) Positional distribution of HLR1 motifs within the set of promoter sequences. A background model was created by permuting (n = 100) the PSWM columns of HLR1 (Figure S1) and detecting occurrences of these random motifs in all promoters of *Synechocystis* 6803 (binwidth = 5 nt; relative motif scores ≥0.90). Throughout the analyses, the same parameters were applied for the background model as well as for HLR1.

(B) Two distinct locations of the HLR1 motif correlate with activation or repression under HL (Figure S2). Promoter sequences were separated before this analysis according to their response to a shift to HL [$\log_2$(HL/median) ≥ 0 or <0]; their density was plotted against their relative distance to the TSS (binwidth = 5 nt; relative motif scores ≥0.90), and enriched areas were defined (density threshold ≥99%), referring to the centered binding sites. The quality of the HLR1 elements from each enriched area was rated by ranking their relative motif scores (output from TFBSTools) against the set of generated background motifs (total rank) and the correlation between the relative expression under HL.

(C) Ranking the relative expression against the HLR1 motif score. A combined rank was calculated for each motif (HLR1 + background), and probabilities were obtained from the distribution of the motifs' combined ranks.

(D) Comparison of the combined HLR1 ranks against their respective probabilities.

Interestingly, similar peak patterns as those observed under HL were detected for cold (15°C) and iron depletion (–Fe) conditions (Figure S2), which is consistent with the fact that the RpaB/Hik33 two-component system acts as a redox sensor for several external stimuli and controls the electron transfer routes, especially in cold-signal transduction (Murata and Los, 2006).

The Combination of Computational Motif Detection, dRNA-Seq Expression Data, and Functional Enrichment Analysis Reveals a Large and Complex RpaB Regulon

The following three criteria were used to filter the HLR1 occurrences in the two distinct peak areas: (1) a probability threshold ≥95%, (2) a relative motif score ≥0.90, and (3) a functional enrichment score >1. At least one of these criteria had to be met for inclusion, yielding a list of 98 activated genes (under the control of 43 promoters) and 196 repressed genes (under the control of 124 promoters) (Table S3). From these, three genes are in both categories, yielding a list of 291 high-ranking members of the RpaB regulon.

The ranked motif scores correlated well with the relative expression of the associated promoters under HL (Figure 2C). Accordingly, the combined rank of motif score and relative expression allowed the computation of a probability for each HLR1/target to be regulated by RpaB (Figure 2D). The probability estimation was generated from the distribution of the background.

Functional enrichment analyses were conducted for the filtered TUs and those down to a probability ≥75% (cf. Figure 2D) using DAVID 6.7 (Huang et al., 2009a, 2009c; 2009b) (Figure S3, Table S2). Targets that were predicted to be repressed by RpaB were enriched in genes with a wide range of functionalities, such as nitrate assimilation, circadian clock, GTP binding, PSII reaction center subunits, and components of associated photosynthetic electron transport chains (Figure S3A). In contrast, genes predicted to be activated

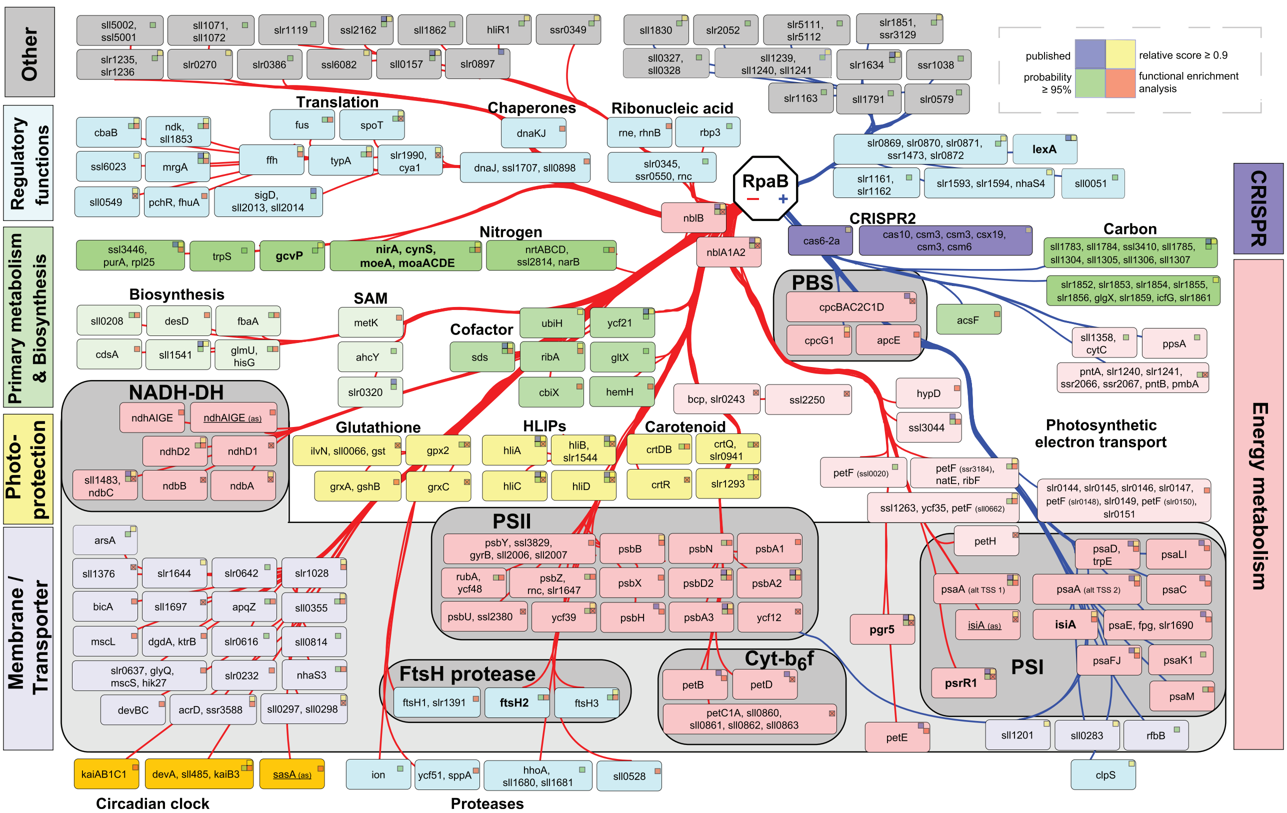

Figure 3. RpaB Regulon of High Probability

All RpaB targets detected by at least one criterion are displayed. A set of up to four squares indicates if the regulation was previously published (blue square), if the probability was ≥95% (green square), if the relative motif score was ≥0.90 (yellow square), and a functional enrichment score of ≥1 (red square). A "x" sign within the red square indicates manual curation due to incomplete database annotation. Putative ncRNAs/asRNAs that have not been further described in the literature are not displayed. The targets were arranged according to their predicted regulation by RpaB and colored according to their membership in functional groups or complexes (for further information about the individual target genes see Table S3; for the total number of RpaB target genes predicted by the multiple approaches see Figure S4). Promoters of targets in boldface letters were selected for experimental analysis, and underlined targets indicate asRNAs such as isiA (as), which is also known as IsrR (Dühring et al., 2006).

by RpaB were enriched for encoding subunits of PSI or the PBS (Figure S3B) and also included *isiA* and *lexA*, and, with the CRISPR2 system, one of the three native CRISPR-Cas systems present in this organism (Scholz et al., 2013).

Using conservative parameter settings, the final set of putative RpaB targets encompassed 188 promoters (Table S3, Figure S4). Of these, 166 control the expression of protein-coding genes and 22 control non-coding TUs. The predicted regulon included 36 of 39 genes or operons previously shown to be under RpaB control in *Synechocystis* 6803 (Figure S4), which validated the performance of our approach. Hence these results raised the number of putative RpaB targets in *Synechocystis* 6803 by approximately 5-fold for all promoters. The three genes or operons that were not identified lacked a TSS in our dataset (*slr0897*), the reported motif differed too much from the HLR1 model employed here (*petE/sll0199*), or the distance to the TSS was higher than that allowed in this analysis (*psbH/ssl2598*). Putative targets were not restricted to the chromosome but were also found on plasmids, suggesting the deep integration of those genes in the regulatory network.

To gain more information about different functionalities, we split the full set of predicted target genes into subclusters (Figure 3) based on functional enrichment analysis. Genes that are important for photoprotection (encoding HLIPs, carotenoid biosynthesis, glutathione/glutaredoxin), photorespiration or synthesis of C1 compounds and cofactors (*gcvP*), photosynthetic electron transport (*petF1-3*, *petE*, *pgr5*), hydrogenase formation (*hypD/slr1498*), cofactor biosynthesis (heme and porphyrin, quinones, riboflavin), nitrogen

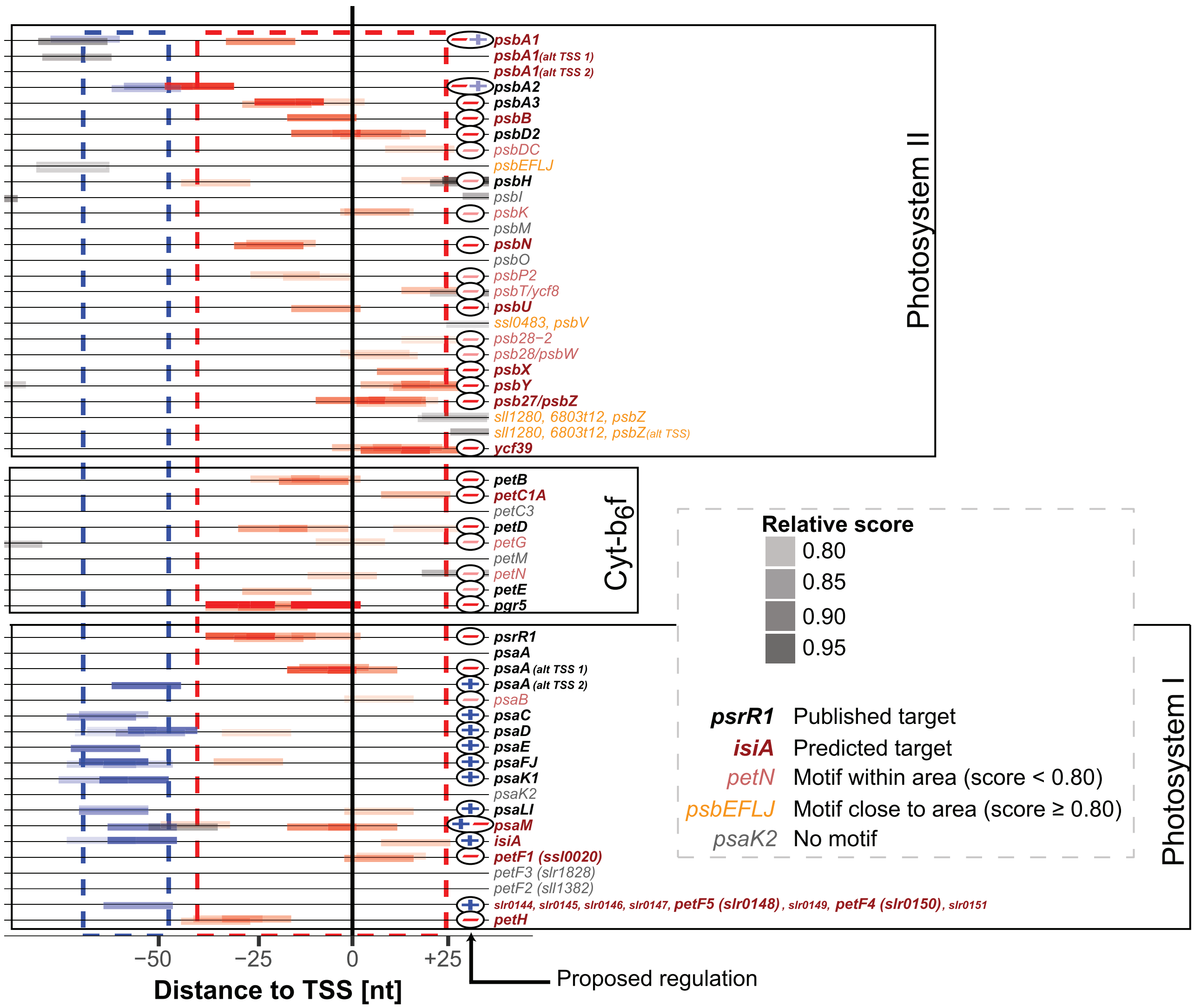

Figure 4. HLR1 Motifs within Promoters of the Photosynthetic Apparatus

Detected HLR1 motifs (score ≥0.75) were plotted against their distance to the corresponding TSS and colored according to the deduced regulation (blue, activation by RpaB; red, repression by RpaB under LL; gray, regulation was not deduced because motif was outside the relevant two regions). The saturation of the motif reflects the consensus with the input motif. The prominent + or – symbols indicate the resulting regulation.

assimilation, and the circadian clock were restricted to the repressing branch of RpaB, consistent with the higher demand for these activities under HL. In addition, many genes encoding stress-related regulatory proteins such as proteases, RNases, chaperones, and GTPases were predicted repressed targets, including three of the four genes encoding subunits of FtsH protease complexes.

A Specific View on Photosynthesis-Related Genes Reveals the Antagonistic Regulation of Most PSII and cytb$_6$f versus PSI Genes by RpaB Binding to Different HLR1 Positions

With a few exceptions, most PSII genes possess an HLR1 within or close to the area where RpaB acts as a repressor, suggesting coordinated co-downregulation via RpaB (Figure 4). Similar observations were made for several genes of the cytochrome b_6f complex and soluble electron acceptors (such as *petE*, *pgr5*, *petF*). On the contrary, most PSI genes harbor an HLR1 in the area where RpaB acts as an activator (Figure 4). A few examples, for which regulation cannot be intuitively inferred, possess complex promoter organization, such as in the case of *psaA* (Takahashi et al., 2010), or multiple instances of an HLR1 motif, as for *psbA1*, *psbA2*, and *psaM* (Figure 4). The *isiA*-IsrR pair is very intriguing: IsrR is the antisense RNA (asRNA) controlling the accumulation of *isiA* mRNA (Dühring et al., 2006). Both promoters have an identical HLR1 element. However, this element is in a repressing position for IsrR and in an activating position in the *isiA* promoter.

Members of the RpaB Regulon Stimulated by HL Have Functions in Cyclic Electron Flow, Photorespiration and Nitrogen Assimilation

The *pgr5* gene is strongly induced when cells are exposed to HL or CO_2 limitation (Kopf et al., 2014). This gene encodes a homolog of PGR5 (proton gradient regulation 5) in *Synechocystis* 6803 (Yeremenko et al., 2005), which is involved in antimycin A-sensitive electron flow from PSI to the plastoquinone (PQ) pool in plants and algae (Munekage et al., 2002; Saroussi et al., 2016). The *pgr5* promoter possesses twin HLR1 boxes, HLR1a and HLR1b, covering the −35 to −10 elements and the first transcribed nucleotide (Figure 5A). ChAP assays utilizing 12xHis-tagged RpaB from an LL-grown culture yielded 32% recovery of this promoter fragment, whereas this number dropped to ~5% at 5 min after transfer to HL and recovered to only 11% at 15 min after the shift, which was even lower than the negative control (Figure S5). In promoter fusion experiments, the native P_{pgr5} promoter mediated a rapid induction of luciferase fluorescence upon the shift from LL to HL. This promoter de-repression was consistent with the rapid induction of *pgr5* mRNA accumulation in the wild-type (WT) 5 min after the shift from LL to HL, shown here by northern blot hybridization and in microarray expression data taken from the CyanoEXpress database (Hernandez-Prieto and Futschik, 2012). Mutation of HLR1b abolished reporter gene expression, whereas mutation of HLR1a alone or of both motifs together led to a more pronounced peak upon transfer from LL to HL (Figure 5A), pointing to additional regulatory mechanisms. It should be noticed that *pgr5* was the most differentially regulated gene in a recently found regulatory mechanism involving the protein Slr1658 (Zer et al., 2018). In *slr1658* disruption mutants, *pgr5* was upregulated by about three orders of magnitude, but no details are known about the respective signaling chain or response regulator (Zer et al., 2018).

Therefore electrophoretic mobility shift assays (EMSAs) were performed, which showed direct binding of RpaB to the native sequence. Binding was still detectable with individual HLR1a or HLR1b mutants but completely abolished when HLR1a and HLR1b were jointly replaced (Figure 5A).

The *slr0293/gcvP* gene encodes the P-protein, one of four subunits of the glycine decarboxylase complex (Eisenhut et al., 2006) involved in the plant-like photorespiratory C2 cycle metabolizing poisonous 2-phosphoglycolate (2-PG), which is a by-product of the bifunctional ribulose-1,5-bisphosphate carboxylase/oxygenase activity. Therefore the enhanced expression of *gcvP* with increased irradiance is sensible and was observed by northern blot hybridization here as well as in microarray expression data from the CyanoEXpress database (Figure 5B). The *gcvP* promoter possesses twin HLR1 boxes. HLR1a covers the −10 element and the region up to −2 of the TSS, whereas HLR1b is located within the 5′ UTR (Figure 5B). ChAP assays using RpaB from an LL-grown culture yielded 38% recovery of this promoter fragment. This number dropped to ~10% at 5 min after transfer to HL and recovered to 22% at 15 min after the shift. In promoter fusion experiments, the native P_{gcvP} promoter mediated an induction in luciferase fluorescence upon a shift from LL to HL within 30 min. Joint mutations of HLR1a and HLR1b abolished reporter gene expression, consistent with EMSA data demonstrating the lack of RpaB binding to the fragment when both sites were mutated (Figure 5B).

The FtsH2 protease, which is important for PSII repair (Komenda et al., 2006), is also controlled by RpaB. P_{ftsH2} possesses a single HLR1 overlapping the TSS and the −10 element (Figure 5C), suggesting a repressing function under LL. Indeed, northern hybridization demonstrated the induction of *ftsH2* mRNA accumulation in the WT upon the shift from LL to HL, but the initial level was higher than for *pgr5*. ChAP assays yielded 27% recovery of this promoter fragment, whereas this number dropped to ~15% at 5 min after transfer to HL, below the negative control value obtained with the *glnB* promoter (Figure S5), suggesting actual RpaB binding. Binding was directly confirmed in EMSA assays with the native promoter sequence, whereas it was abolished when the motif was mutated (Figure 5C). Reporter gene assays confirmed the inducibility by HL. The HLR1 mutation led to reduced, but still detectable, HL-inducible expression of the reporter gene. We conclude that P_{ftsH2} is under RpaB control and that the existing second TSS secured the lower, albeit still detectable, regulation when HLR1 was mutated.

We chose the promoter of PsrR1 as a positive control (Georg et al., 2014; Kadowaki et al., 2016). P_{PsrR1} possesses an HLR1 spanning the region from the −35 to the −10 element (Figure 5D). Indeed, ChAP assays

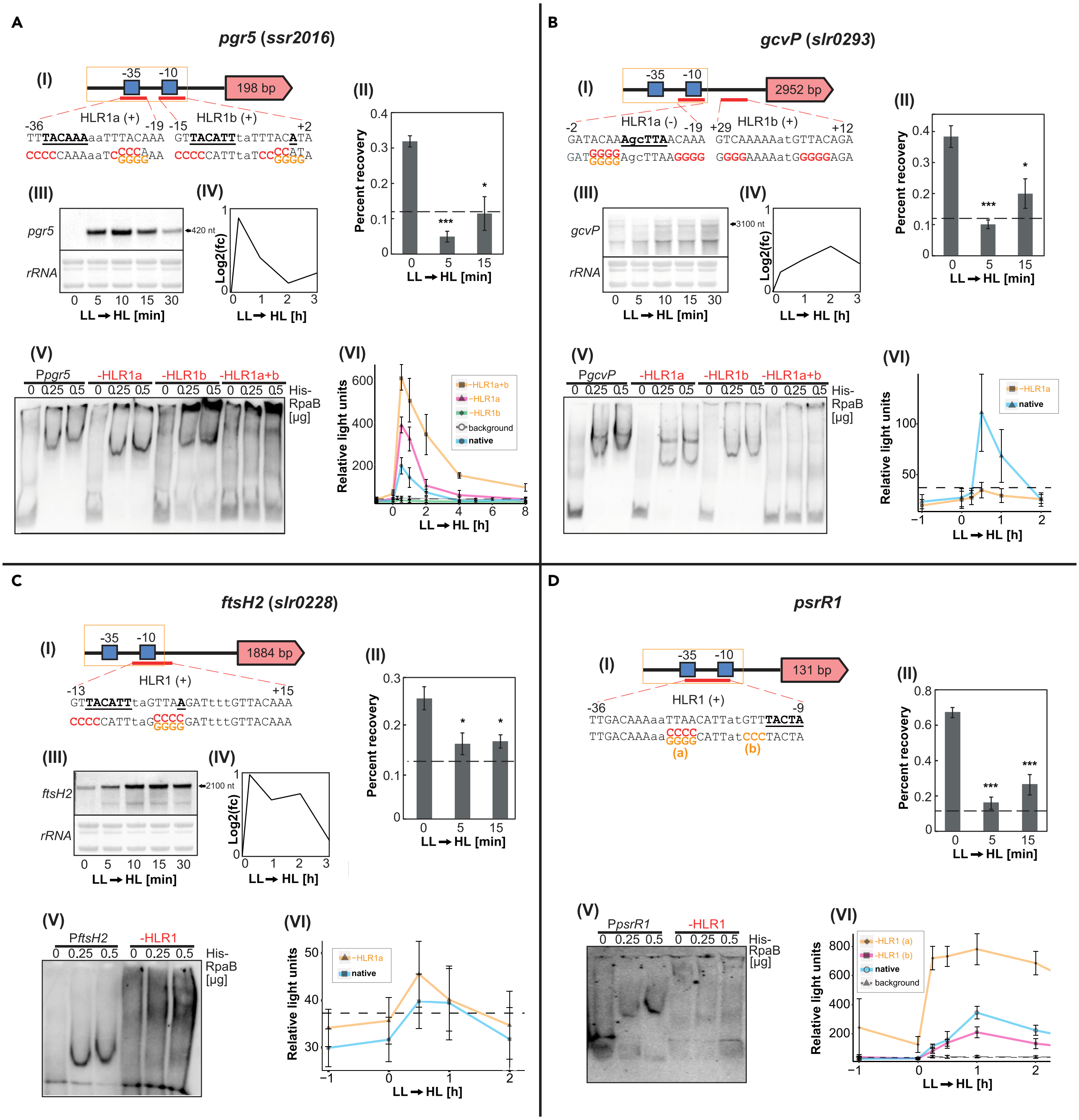

Figure 5. Experimental Validation of Selected Potential Target Genes Predicted to be Repressed by RpaB

(A) *pgr5* (*ssr2016*).

(B) *gcvP* (*slr0293*).

(C) *ftsH2* (*slr0228*).

(D) *psrR1* serving as a positive control (Kadowaki et al., 2016) for the conducted experiments. (I) Schematic representation of individual promoters. Red bars give the HLR1 location; (+) or (−) signs indicate the orientation on the forward or reverse strand. The sequences are given in capital letters underneath; other promoter elements and the TSS are underlined and in boldface. Introduced point mutations are marked in red for the EMSA (III) and in orange for the luciferase assay (VI). (II) ChAP analysis. Percent recovery after the shift to HL. The dashed line resembles the maximum percent recovery that was obtained from the negative control (Figure S5). Data represent means ± SD from three independent experiments. Statistical analysis was performed using two-tailed unpaired Student's t test (*p < 0.05, ***p < 0.001) of samples before and after HL induction. (III) Northern blot. Transcript levels after the shift to HL. (IV) Expression profile. Relative expression after shift to HL, taken from the CyanoEXpress database (Hernandez-Prieto and Futschik, 2012). (V) Electrophoretic mobility shift assays (EMSA). Binding of purified His-RpaB (also binding of His-FurA in the case of *isiA*) (Figure S6) to the native and mutated promoters. The

Figure 5. *Continued*

sites of the introduced mutations are depicted in red in the HLR1 shown in (I). (VI) Luciferase reporter assays. Absolute luminescence (relative light units) under HL exposure (alternatively, nitrogen depletion + HL exposure in the case of *nirA* and iron depletion + HL exposure in the case of *isiA*, refer to Figure 6). Data represent means ± SD from triplicates of two biological replicates and from at least three independent experiments. The native promoters that were used are boxed in orange in part (I). The background luminescence (average background = dashed line) originated from a strain containing only the decanal-producing plasmid, used as a negative control. Sequences of desoxyoligonucleotides used for the construction of recombinant plasmids are given in Table S4.

yielded 65% recovery of this promoter when protein extracts from LL-grown cultures were applied, whereas this number dropped to less than 20% at 5 min after transfer to HL and recovered to 25% at 15 min after the shift. Moreover, EMSAs showed direct binding of RpaB to the native sequence, whereas binding was not observed when the HLR1 motif was mutated. In promoter-reporter gene fusion assays, we observed rapid de-repression upon the shift to HL and even stronger de-repression when the HLR1 motif was replaced. In contrast, mutation of the −10 element led to low expression and almost no detectable light induction (Figure 5D). These facts corresponded well to the known regulation of this sRNA (Georg et al., 2014).

HLR1 Motifs in Complex Promoter Architectures Suggest the Integration of Redox Signaling with Different Environmental Signals Transmitted by Other Transcription Factors

Several putative RpaB-binding sites were detected in promoters that are known to be regulated by other transcription factors such as Fur, LexA, or NtcA. Hence the promoters of the *isiA*, *nirA*, and *lexA* genes were examined to gain insight into the cross-regulation between RpaB and other transcription factors. The gene *isiA* encoding the chlorophyll-binding protein CP43′ or IsiA (iron stress-induced protein A) is repressed under iron-replete growth conditions by the ferric uptake regulator Fur (Vinnemeier et al., 1998), and it is de-repressed under iron starvation (Burnap et al., 1993; Laudenbach and Straus, 1988). The *isiA* promoter was predicted with high confidence as an RpaB target. The HLR1 motif finishes only 5 nt upstream of one of the two Fur-binding elements (Figure 6A). RpaB binding was confirmed by the ChAP assay; also recovery of the native promoter fragment dropped 5 min after the shift to HL. Binding of both transcription factors, RpaB as well as Fur, to the expected promoter motifs was confirmed by EMSA. Although the HLR1 motif was identified in the activating position, we could not detect *isiA* transcripts under LL conditions (Figure 6A [III], +Fe). However, after incubation under iron-deplete conditions for 48 h, high transcript accumulation was detected, with a slight decrease after the shift to HL (Figure 6A [III], 48 h −Fe). The reason for this finding is its parallel repression by Fur, as validated by the reporter gene assays. When the cells were starved for iron, gene expression from the native promoter increased linearly for 36 h, whereas mutation of the Fur box caused very high expression before iron was removed, consistent with the role of Fur as a repressor. However, when HLR1 was mutated, no expression could be detected at all, even if the Fur box was mutated in parallel. This result suggested that RpaB was required for the high-level expression of *isiA* under iron-limiting conditions. Consistent with this interpretation, the shift from LL to HL led to a remarkable decrease in gene expression with both the native and Fur box-mutated promoter variants, followed by an increase when the cells were shifted back (Figure 6A [VI]).

The *nirA* gene encoding nitrite reductase belongs to the core regulon controlled by global nitrogen regulator NtcA (Giner-Lamia et al., 2017, p.). The NtcA box within P_{nirA} overlaps the HLR1 by 5 nt (Figure 6B [I]). Under nitrogen-replete growth conditions, *nirA* transcript levels declined immediately after exposure to HL, and then increased to the level higher than that under LL (Figure 6B [III and IV]). Such tendency was also observed in promoter activity under nitrogen-depleted conditions (Figure 6B [VI]). Point mutations in either HLR1 or NtcA boxes resulted in decreased luminescence relative to the natural promoter (Figure 6B [VI]). EMSAs showed a simple band pattern and specific binding of RpaB to the HLR1 sequence in P_{nirA}, whereas binding was abolished when HLR1 was mutated.

LexA is a highly conserved transcription factor throughout the bacterial domain and frequently functions as a repressor of SOS response-related genes involved in DNA repair (Butala et al., 2009). In *Synechocystis* 6803, however, LexA has been reported to act as a global regulator binding to the promoters of genes contributing to various cellular functions, such as hydrogenase activity (Oliveira and Lindblad, 2005), bicarbonate transport (Lieman-Hurwitz et al., 2009), twitching motility (Kizawa et al., 2016), glucosylglycerol accumulation (Kizawa et al., 2016), and fatty acid biosynthesis (Kizawa et al., 2017). The promoter of *lexA* harbors a single HLR1 in the activating position (Figure 6C (I)). Our experimental data show that RpaB

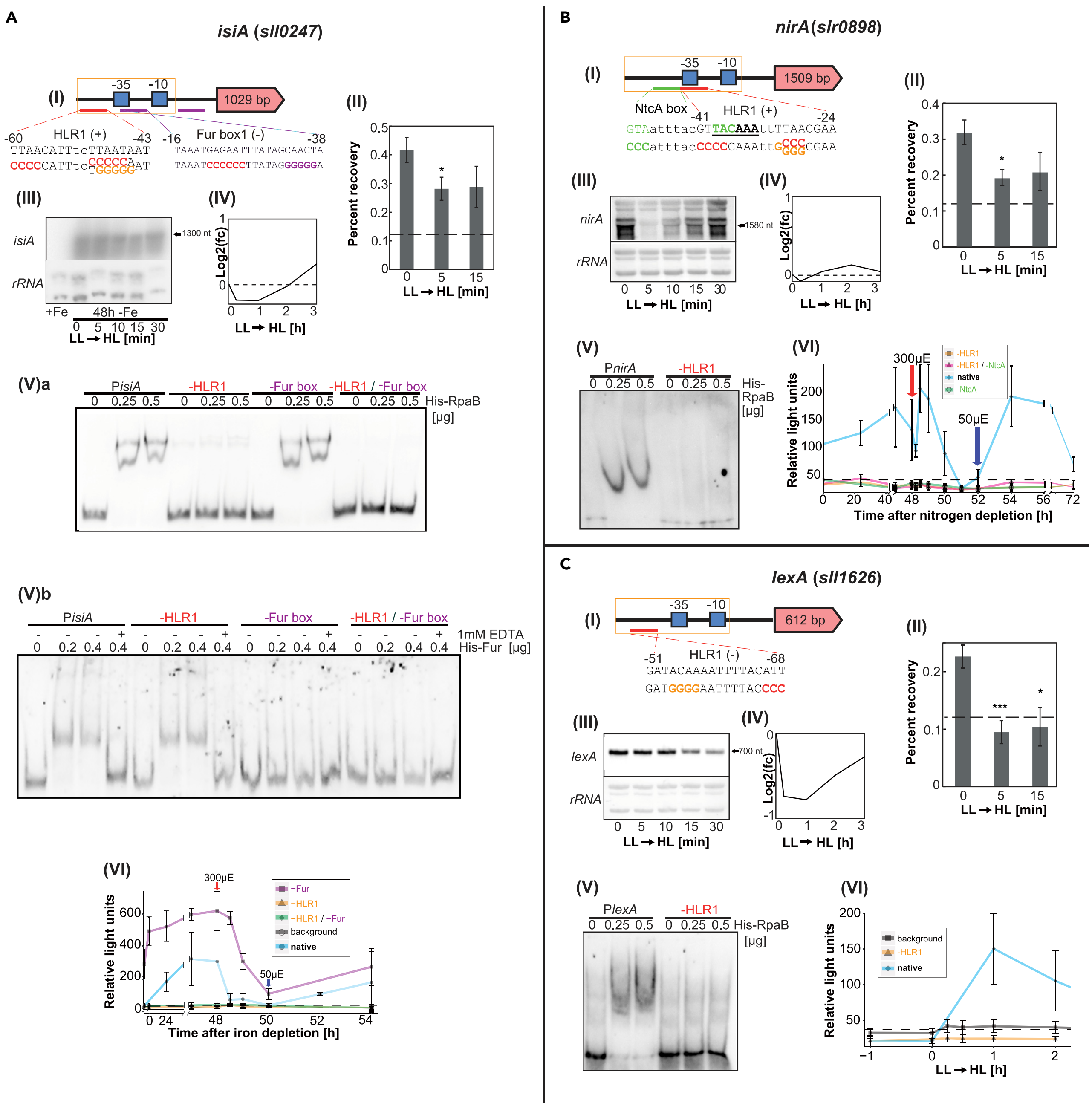

Figure 6. Experimental Validation of Selected Potential RpaB Target Genes Showing Cross-regulation with Other Transcriptional Regulators

(A) *isiA (sll0247).* The Fur boxes were taken from publication (Kunert et al., 2003).

(B) *nirA (slr0898).* The NtcA box was taken from publication (Giner-Lamia et al., 2017).

(C) *lexA (sll1626).* (I–VI) Refer to explanations in Figure 5.

bound to P_{lexA} with extracts from LL-grown cells, whereas this binding was lost 5 min after transfer to HL and mutation of HLR1 within P_{lexA} prevented RpaB binding (Figure 6C [II and V]). Moreover, fusion of the native promoter to the reporter did indeed yield fluorescence, whereas HLR1 mutation prevented it. Hence activation of P_{lexA} by RpaB under LL was validated. Consistently, decreasing *lexA* transcript levels were observed after transfer to HL (Figure 6C [III and IV]). However, *lexA* promoter activity increased after 1 h of HL exposure (Figure 6C [VI]). This increase in promoter activity was not observed when a mutation was introduced into HLR1 (Figure 6C [VI]), indicating that this increase was due to the re-binding of

RpaB to HLR1. Although LexA has been suggested to be negatively auto-regulated (Kizawa et al., 2017), our results did not show any clue for self-repression of the *lexA* gene.

The RpaB Regulon Is Complex and Partially Conserved among Species

Our results predict a functionally far more complex regulon controlled by RpaB than known thus far. ChIP sequencing (ChIP-seq) analysis previously performed in *S. elongatus* that included RpaB (Piechura et al., 2017) allows the comparison of our dataset across species borders. Only 117 of the 291 high-ranking genes proposed to belong to the RpaB regulon in *Synechocystis* 6803 have a matching homolog in *S. elongatus*. From these, 29 were also found by ChIP-seq. Most of these genes are associated with photosynthesis (*apcE*, *cpcB/G1*, *petB/C1*, *psaA/D/E/I/K1*, *psbA1/B*), some have photoprotective or regulatory functions (*ftsH2/H3*, *hliA/C*, *nblA2*, *ndbA*, *pds*, *sigD*), and several are insufficiently characterized (*sll0195*, *sll1071*, *sll1481*, *slr0642*, *slr1634*, *ssl3044*, *ssl0349*, *ycf21*, *ycf39*). Although some promoters may have been missed by the ChIP-seq analysis, this comparison shows that the functionality of the RpaB regulon goes beyond photosynthetic gene functions in both species.

DISCUSSION

Extension of the RpaB Regulon

Our results substantially increase the number of known RpaB-regulated promoters in *Synechocystis* 6803, from 37 to at least 167 for protein-coding genes or operons and from 1 to 22 non-coding RNAs. To infer the regulon controlled by RpaB, we analyzed the positional distributions of RpaB-binding sites and the expression profiles of the regulated genes and performed functional enrichment analysis. For seven selected examples, we performed reporter gene assays, ChAP assay, and EMSA assay and measured mRNA accumulation by northern hybridizations. The results from the luciferase reporter gene assays revealed inducibility as early as 30 min after exposure to HL for promoters that were predicted to be repressed by RpaB under LL (*ftsH2*, *pgr5*, *gcvP* and *psrR1* for control), hence confirming the validity of our approach.

RpaB as a Key Regulator for Redox Regulation and Acclimation to HL

Several putative target genes associated with photosynthetic functions or electron transfer were identified. These findings add to the known role of RpaB as a key regulator of many essential subunits of the photosynthetic apparatus and strongly support that RpaB is involved in redox regulation and acclimation to HL. Our data demonstrate the involvement of RpaB in the control of *pgr5/ssr2016*, which is involved in cyclic electron flow, and in the expression of *gcvP/slr0293*, encoding the glycine decarboxylase P-protein, one of the four subunits of the glycine decarboxylase complex. The finding of dual HLR1 boxes in the *pgr5/ssr2016* promoter is intriguing. The twin HLR1 elements likely ensure tight regulation under LL, similar to the role of the twin Fur boxes in the *isiA* promoter (Kunert et al., 2003). The encoded Pgr5 protein is involved in cyclic electron flow from PSI to the PQ pool in cyanobacteria, plants, and algae alike (Yeremenko et al., 2005). The major function of cyclic electron flow is to balance ATP/NADPH ratios and prevent PSI photoinhibition (Shikanai, 2014). Therefore it makes perfect sense that *pgr5* is controlled by RpaB. However, PSI photoinhibition is also prevented by Mehler-like reactions mediated by the Flv1 and Flv3 proteins (Allahverdiyeva et al., 2013), but the genes encoding these proteins (*sll1521* and *sll0550*) were not found here, suggesting a more specific role for RpaB in state transition and cyclic electron flow. Further predicted target genes encode components of the NADH dehydrogenase complex such as *ndhD2/slr1291* and *ndhAIGE* (*sll0519-sll0522*), consistent with the suggested link between these complexes and cyclic electron transport (Gao et al., 2016; Liu et al., 2012; Mullineaux, 2014). Other functionally connected targets involve subunits of the cytochrome b_6f complex, plastocyanin (*petE*), five ferredoxins (*ssl0020*, *sll0662*, *ssr3184*, *slr0148*, *slr0150*) (fed1-5 = all plant-like ferredoxins), as well as *petH*, encoding the ferredoxin-NADP(+) oxidoreductase, bacterioferritin (Bcp/Slr0242), and its associated ferredoxin (Ssl2250), which were reported to be involved in resistance to oxidative stress by utilizing thioredoxin as a reductant (Clarke et al., 2010). Thioredoxin was shown to directly influence the RpaB redox state (Kadowaki et al., 2015), and therefore RpaB might indirectly control its own activity via the downregulation of *bcp* and *ssl2250*. Altogether, RpaB controls six of nine ferredoxins present in *Synechocystis* 6803 (Cassier-Chauvat and Chauvat, 2014). These findings illustrate the importance of regulation of the electron distribution within and downstream of photosynthesis via RpaB.

Photorespiratory 2-PG metabolism is essential in cyanobacteria and especially important during HL acclimation (Eisenhut et al., 2008; Hackenberg et al., 2009). The production of 2-PG promotes the accumulation of glycine in HL, which is toxic in high concentrations (Eisenhut et al., 2007). Therefore the glycine cleavage complex is important for HL acclimation processes as well. Redox regulation of *gcvP*, encoding the P-protein subunit of this complex, was reported (Hasse et al., 2013), which, according to our data, is performed by RpaB. As proposed for P*pgr5*, the possession of two HLR1 elements could ensure a tight regulation. The cellular antioxidant defense system consists of various mechanisms to maintain redox homeostasis, which is crucial to cope with stress conditions, such as HL. RpaB seems to regulate most genes of the glutathione/glutaredoxin system, relevant to prevent photooxidative damage. GrxA and GrxC were reported to be the only HL-inducible glutaredoxins, serving as electron acceptors of glutathione (Sánchez-Riego et al., 2013).

Cross-regulatory Effects between RpaB and Other Regulatory Mechanisms

Our results for the genes *isiA* and *nirA* point to cross-regulation with the transcription factors Fur and NtcA, respectively. Mediated by Fur, many cyanobacteria respond to iron starvation by expressing IsiA (Burnap et al., 1993; Laudenbach and Straus, 1988). IsiA initially forms antenna rings around trimeric PSI (Bibby et al., 2001) and likely serves as an extra light-harvesting complex, whereas it functions later in the dissipation of excess light energy (Ihalainen et al., 2005; Yeremenko et al., 2004) and exerts a protective function (Havaux et al., 2005). Repression of *isiA* by Fur under iron-replete growth conditions was validated by the high luciferase expression measured when the Fur box was mutated and the fact that the native promoter became induced 24 h after the removal of iron ions (Figure 6A [VI]). In contrast, mutagenesis of the HLR1 site completely abolished *isiA* expression, even under iron-deplete conditions, demonstrating the function of RpaB as an activator of *isiA* gene expression. Our identification of RpaB as an activator of *isiA* gene expression adds up to the tight repression by Fur and the asRNA IsrR (Dühring et al., 2006), which was predicted to be repressed by RpaB at LL (Figure 3, Table S3). Therefore the here suggested involvement of RpaB in the transcriptional regulation of *isiA*, and inversely in the control of its asRNA IsrR, adds a regulatory dimension that has been previously missing.

RpaB control over the glutathione/glutaredoxin system illustrates its interface with nitrogen metabolism, which is important for enhancing the electron sink capacity. Cross-regulation with NtcA in the control of *nirA/slr0898*, encoding ferredoxin-nitrite reductase, also fits this picture. Binding of RpaB to the *nirA* promoter was clearly shown; however, the HLR1 is at an intermediate position at $-41 \sim -24$, which is still compatible with activation by RpaB. Therefore the observed decline after HL shift in the amount of the *nirA* transcript in the presence of combined nitrogen (Figure 6B [III] and [IV]) and in the promoter activity in the absence of combined nitrogen (Figure 6B [VI]) can be explained by the release of RpaB. An overcompensation observed after initial decline was likely mediated by NtcA. Upon the inverse shift from HL to LL, the observed increase in activity was solely due to activation by RpaB. Hence the *nirA* promoter is co-stimulated by NtcA and RpaB. However, an asRNA overlapping the first codons and 5′UTR of *nirA* has been detected (Giner-Lamia et al., 2017; Kopf et al., 2014) and may contribute to the control of mRNA stability and the efficiency of translation in the native situation.

RpaB also indirectly influences the activity of other transcription factors via the regulation of FtsH genes. The predicted target genes *slr0228* and *slr1604* encode the FtsH2/3 protease complex, which is important for PSII repair (Komenda et al., 2006). It is intriguing that the FtsH2 protease is also required for the induction of inorganic carbon acquisition complexes in *Synechocystis* 6803, acting upstream of the transcription factor NdhR (Zhang et al., 2007), and that the FtsH1/3 heterocomplex controls the level of Fur (Krynická et al., 2014). All three genes (*ftsH1*, *ftsH2*, *ftsH3*) are repressed by RpaB (Figure 3).

The Central Regulatory Role of RpaB and the Factors Controlling It

Multiple signals converge though the Hik33-RpaB two-component system (Figure 7). Hik33 acts as a multi-stress sensor to several environmental stresses such as low temperature, hyperosmolarity, high salinity, high light, oxidative stress, and certain nutrient limitations (Kanesaki et al., 2007; Marin et al., 2003; Mikami et al., 2002; Suzuki et al., 2000; Tu et al., 2004; van Waasbergen et al., 2002). The outcome of the Hik33-RpaB interaction is not entirely clear; in *S. elongatus* the phosphorylation level and DNA-binding activity of RpaB decrease in response to HL exposure (López-Redondo et al., 2010; Moronta-Barrios et al., 2012). DNA-binding activity of RpaB is reduced upon shift to HL clearly also in *Synechocystis* 6803 (cf. panels [II] in Figures 5 and 6). RpaB is an important component in the output from the circadian clock. ChIP-seq analysis suggested that RpaB phosphorylation enables DNA-binding activity of RpaB, which functions as an activator of dusk gene expression (Piechura et al., 2017). In addition, the circadian clock output regulator

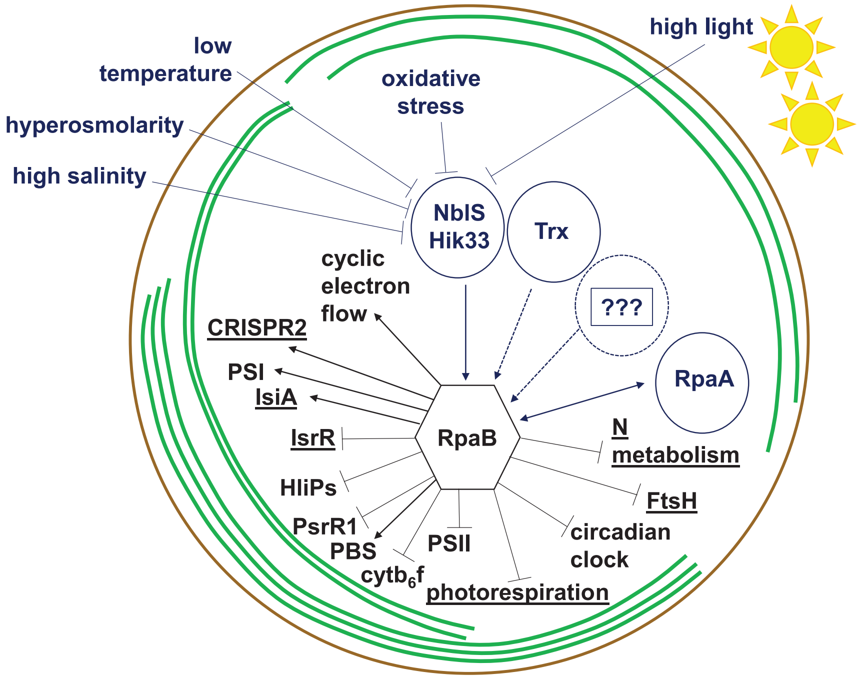

Figure 7. Regulation through the Hik33-RpaB System

RpaB activates transcription of genes encoding phycobilisome proteins, proteins involved in cyclic electron flow, PSI proteins, and proteins that can be associated with PSI under certain conditions such as IsiA, and also the CRISPR2 system. RpaB represses several PSII genes, the cytb$_6$f system, ferredoxins, genes with protective functions (HLIPs, photorespiration), FtsH proteases, enzymes and transporters involved in nitrate and nitrite metabolism and some riboregulators of PSI genes such as PsrR1 or IsrR, and many other genes and subsystems not shown here. Previously not associated functional classes or genes predicted in this work are underlined. For further details, see Figure 3. Signal input to RpaB (colored blue). The histidine kinase Hik33 (also called NblS) and RpaB form a two-component regulatory system. Hik33 acts as a multi-stress sensor to several environmental stresses (Kanesaki et al., 2007; Marin et al., 2003; Mikami et al., 2002; Suzuki et al., 2000; Tu et al., 2004; van Waasbergen et al., 2002). All these stresses affect the membrane fluidity or the redox state of the cell sensed by Hik33. Exposure to high light intensities leads to a lowered phosphorylation level of RpaB and diminished DNA-binding activity in *S. elongatus* (López-Redondo et al., 2010; Moronta-Barrios et al., 2012). The circadian clock output regulator RpaA interacts with RpaB in *S. elongatus* (Espinosa et al., 2015; Gutu and O'Shea, 2013) and *Synechocystis* 6803 (Köbler et al., 2018), integrating circadian clock control with redox regulation. *In vitro* studies suggested that the redox state of the photosynthetic electron transport chain is transmitted to RpaB via thioredoxins (Kadowaki et al., 2015). Additional input signals may exist, indicated by the dashed lines and question marks.

RpaA was found to interact with RpaB in *S. elongatus* (Espinosa et al., 2015; Gutu and O'Shea, 2013) and *Synechocystis* 6803 (Köbler et al., 2018). *In vitro* studies suggested that the redox state of the photosynthetic electron transport chain is transmitted to RpaB via thioredoxins (Kadowaki et al., 2015) and that additional regulatory inputs may exist.

Together with previous data, the results of this work show that RpaB is of crucial and central relevance for the light and redox-dependent remodeling of the photosynthetic apparatus, various electron transfer chains, state transitions, and, overall, for the light acclimation of photosynthetic cyanobacteria. The RpaB regulon encompasses many additional genes that are more loosely or not at all associated with the photosynthetic machinery (Figure 7). RpaB is involved in the control of carbon and nitrogen primary metabolism and the circadian clock and exerts cross-regulation with other transcription factors such as NtcA or FurA. The size and importance of the controlled regulon characterize RpaB as one of the most crucial transcriptional regulators in oxyphototrophic microorganisms.

Limitations of the Study

With regard to the signaling toward RpaB, thioredoxin was found to directly influence the RpaB redox state (Kadowaki et al., 2015), making it a candidate for transmitting the redox state of the photosynthetic electron chain to RpaB. However, the interaction with thioredoxin was studied only *in vitro*, so its biological relevance cannot properly be evaluated at the current time. Regarding the mechanism by which RpaB activates transcription, it is likely that RNAP is "recruited," possibly via an interaction with the C-terminal domain of the RNAP α subunit, in analogy to the mechanism by which the enterobacterial Crp activates transcription (Lawson et al., 2004). However, information on the different types of promoters, regulatory elements, and transcription factors in cyanobacteria is still too limited for sound conclusions on the involved mechanisms.

METHODS

All methods can be found in the accompanying Transparent Methods supplemental file.

SUPPLEMENTAL INFORMATION

Supplemental Information can be found online at https://doi.org/10.1016/j.isci.2019.04.033.

ACKNOWLEDGMENTS

We thank Martin Hagemann, University of Rostock, for critical reading of an earlier manuscript version. This work was supported by Grants-in-Aid for Scientific Research (C) from the Ministry of Education, Culture, Sports, Science and Technology (MEXT) to Y.H. and by the Federal Ministry of Education and Research (BMBF) program RNAProNet, grant 031L0164B, to W.R.H. M.R. is a PhD student in the Research Training Group GRK2344, supported by a grant of the Deutsche Forschungsgemeinschaft to W.R.H.

AUTHOR CONTRIBUTIONS

M.R., T.K., and R.N. carried out the molecular genetic and microbiological analyses, M.R. and T.K. constructed and provided mutants and constructs, and M.R. performed the bioinformatics analyses with support by J.G. W.R.H. and Y.H. designed the study, and all authors analyzed data. M.R., W.R.H., and Y.H. drafted the manuscript with contributions from all authors. All authors read and approved the final manuscript.

DECLARATION OF INTERESTS

The authors declare no competing interests.

Received: January 10, 2019
Revised: April 5, 2019
Accepted: April 24, 2019
Published: May 31, 2019

REFERENCES

Allahverdiyeva, Y., Mustila, H., Ermakova, M., Bersanini, L., Richaud, P., Ajlani, G., Battchikova, N., Cournac, L., and Aro, E.-M. (2013). Flavodiiron proteins Flv1 and Flv3 enable cyanobacterial growth and photosynthesis under fluctuating light. Proc. Natl. Acad. Sci. U S A *110*, 4111–4116.

Ashby, M.K., and Mullineaux, C.W. (1999). Cyanobacterial *ycf27* gene products regulate energy transfer from phycobilisomes to photosystems I and II. FEMS Microbiol. Lett. *181*, 253–260.

Bibby, T.S., Nield, J., and Barber, J. (2001). Iron deficiency induces the formation of an antenna ring around trimeric photosystem I in cyanobacteria. Nature *412*, 743–745.

Burnap, R.L., Troyan, T., and Sherman, L.A. (1993). The highly abundant chlorophyll-protein complex of iron-deficient *Synechococcus* sp. PCC7942 (CP43′) is encoded by the *isiA* gene. Plant Physiol. *103*, 893–902.

Butala, M., Žgur-Bertok, D., and Busby, S.J.W. (2009). The bacterial LexA transcriptional repressor. Cell. Mol. Life Sci. *66*, 82–93.

Cassier-Chauvat, C., and Chauvat, F. (2014). Function and regulation of ferredoxins in the cyanobacterium, *Synechocystis* PCC6803: recent advances. Life (Basel) *4*, 666–680.

Clarke, D.J., Ortega, X.P., Mackay, C.L., Valvano, M.A., Govan, J.R.W., Campopiano, D.J., Langridge-Smith, P., and Brown, A.R. (2010). Subdivision of the bacterioferritin comigratory protein family of bacterial peroxiredoxins based on catalytic activity. Biochemistry *49*, 1319–1330.

Cline, M.S., Smoot, M., Cerami, E., Kuchinsky, A., Landys, N., Workman, C., Christmas, R., Avila-Campilo, I., Creech, M., Gross, B., et al. (2007). Integration of biological networks and gene expression data using Cytoscape. Nat. Protoc. *2*, 2366–2382.

Dühring, U., Axmann, I.M., Hess, W.R., and Wilde, A. (2006). An internal antisense RNA regulates expression of the photosynthesis gene *isiA*. Proc. Natl. Acad. Sci. U S A *103*, 7054–7058.

Eisenhut, M., Bauwe, H., and Hagemann, M. (2007). Glycine accumulation is toxic for the cyanobacterium *Synechocystis* sp. strain PCC 6803, but can be compensated by supplementation with magnesium ions. FEMS Microbiol. Lett. *277*, 232–237.

Eisenhut, M., Kahlon, S., Hasse, D., Ewald, R., Lieman-Hurwitz, J., Ogawa, T., Ruth, W., Bauwe, H., Kaplan, A., and Hagemann, M. (2006). The plant-like C2 glycolate cycle and the bacterial-like glycerate pathway cooperate in phosphoglycolate metabolism in cyanobacteria. Plant Physiol. *142*, 333–342.

Eisenhut, M., Ruth, W., Haimovich, M., Bauwe, H., Kaplan, A., and Hagemann, M. (2008). The photorespiratory glycolate metabolism is essential for cyanobacteria and might have been conveyed endosymbiontically to plants. Proc. Natl. Acad. Sci. U S A *105*, 17199–17204.

Eriksson, J., Salih, G.F., Ghebramedhin, H., and Jansson, C. (2000). Deletion mutagenesis of the 5′ *psbA2* region in *Synechocystis* 6803: identification of a putative *cis* element involved in photoregulation. Mol. Cell Biol. Res. Commun. *3*, 292–298.

Espinosa, J., Boyd, J.S., Cantos, R., Salinas, P., Golden, S.S., and Contreras, A. (2015). Cross-talk and regulatory interactions between the essential response regulator RpaB and cyanobacterial circadian clock output. Proc. Natl. Acad. Sci. U S A *112*, 2198–2203.

Gao, F., Zhao, J., Chen, L., Battchikova, N., Ran, Z., Aro, E.-M., Ogawa, T., and Ma, W. (2016). The NDH-1L-PSI supercomplex is important for efficient cyclic electron transport in cyanobacteria. Plant Physiol. *172*, 1451–1464.

Georg, J., Dienst, D., Schürgers, N., Wallner, T., Kopp, D., Stazic, D., Kuchmina, E., Klähn, S., Lokstein, H., Hess, W.R., et al. (2014). The small regulatory RNA SyR1/PsrR1 controls photosynthetic functions in cyanobacteria. Plant Cell *26*, 3661–3679.

Giner-Lamia, J., Robles-Rengel, R., Hernández-Prieto, M.A., Muro-Pastor, M.I., Florencio, F.J., and Futschik, M.E. (2017). Identification of the direct regulon of NtcA during early acclimation to nitrogen starvation in the cyanobacterium *Synechocystis* sp. PCC 6803. Nucleic Acids Res. *45*, 11800–11820.

Gutu, A., and O'Shea, E.K. (2013). Two antagonistic clock-regulated histidine kinases time the activation of circadian gene expression. Mol. Cell *50*, 288–294.

Hackenberg, C., Engelhardt, A., Matthijs, H.C.P., Wittink, F., Bauwe, H., Kaplan, A., and Hagemann, M. (2009). Photorespiratory 2-phosphoglycolate metabolism and photoreduction of O_2 cooperate in high-light acclimation of *Synechocystis* sp. strain PCC 6803. Planta *230*, 625–637.

Hanaoka, M., Takai, N., Hosokawa, N., Fujiwara, M., Akimoto, Y., Kobori, N., Iwasaki, H., Kondo, T., and Tanaka, K. (2012). RpaB, another response regulator operating circadian clock-dependent transcriptional regulation in *Synechococcus elongatus* PCC 7942. J. Biol. Chem. *287*, 26321–26327.

Hanaoka, M., and Tanaka, K. (2008). Dynamics of RpaB-promoter interaction during high light stress, revealed by chromatin immunoprecipitation (ChIP) analysis in *Synechococcus elongatus* PCC 7942. Plant J. Cell Mol. Biol. *56*, 327–335.

Hasse, D., Andersson, E., Carlsson, G., Masloboy, A., Hagemann, M., Bauwe, H., and Andersson, I. (2013). Structure of the homodimeric glycine decarboxylase P-protein from *Synechocystis* sp. PCC 6803 suggests a mechanism for redox regulation. J. Biol. Chem. *288*, 35333–35345.

Havaux, M., Guedeney, G., Hagemann, M., Yeremenko, N., Matthijs, H.C.P., and Jeanjean, R. (2005). The chlorophyll-binding protein IsiA is inducible by high light and protects the cyanobacterium *Synechocystis* PCC6803 from photooxidative stress. FEBS Lett. *579*, 2289–2293.

Hernandez-Prieto, M.A., and Futschik, M.E. (2012). CyanoEXpress: a web database for exploration and visualisation of the integrated transcriptome of cyanobacterium *Synechocystis* sp. PCC6803. Bioinformation *8*, 634–638.

Huang, D.W., Sherman, B.T., and Lempicki, R.A. (2009a). Bioinformatics enrichment tools: paths toward the comprehensive functional analysis of large gene lists. Nucleic Acids Res. *37*, 1–13.

Huang, D.W., Sherman, B.T., and Lempicki, R.A. (2009b). Systematic and integrative analysis of large gene lists using DAVID bioinformatics resources. Nat. Protoc. *4*, 44–57.

Huang, D.W., Sherman, B.T., Zheng, X., Yang, J., Imamichi, T., Stephens, R., and Lempicki, R.A. (2009c). Extracting biological meaning from large gene lists with DAVID. Curr. Protoc. Bioinforma. Chapter 13. https://doi.org/10.1002/0471250953.bi1311s27.

Ihalainen, J.A., D'Haene, S., Yeremenko, N., van Roon, H., Arteni, A.A., Boekema, E.J., van Grondelle, R., Matthijs, H.C.P., and Dekker, J.P. (2005). Aggregates of the chlorophyll-binding protein IsiA (CP43′) dissipate energy in cyanobacteria. Biochemistry *44*, 10846–10853.

Kadowaki, T., Nagayama, R., Georg, J., Nishiyama, Y., Wilde, A., Hess, W.R., and Hihara, Y. (2016). A feed-forward loop consisting of the response regulator RpaB and the small RNA PsrR1 controls light acclimation of photosystem I gene expression in the cyanobacterium *Synechocystis* sp. PCC 6803. Plant Cell Physiol. *57*, 813–823.

Kadowaki, T., Nishiyama, Y., Hisabori, T., and Hihara, Y. (2015). Identification of OmpR-family response regulators interacting with thioredoxin in the cyanobacterium *Synechocystis* sp. PCC 6803. PLoS One *10*, e0119107.

Kanesaki, Y., Yamamoto, H., Paithoonrangsarid, K., Shumskaya, M., Suzuki, I., Hayashi, H., and Murata, N. (2007). Histidine kinases play important roles in the perception and signal transduction of hydrogen peroxide in the cyanobacterium, *Synechocystis* sp. PCC 6803. Plant J. *49*, 313–324.

Kappell, A.D., Bhaya, D., and Van Waasbergen, L.G. (2006). Negative control of the high light-inducible *hliA* gene and implications for the activities of the NblS sensor kinase in the cyanobacterium *Synechococcus elongatus* strain PCC 7942. Arch. Microbiol. *186*, 403–413.

Kappell, A.D., and van Waasbergen, L.G. (2007). The response regulator RpaB binds the high light regulatory 1 sequence upstream of the high-light-inducible *hliB* gene from the cyanobacterium *Synechocystis* PCC 6803. Arch. Microbiol. *187*, 337–342.

Kato, H., Kubo, T., Hayashi, M., Kobayashi, I., Yagasaki, T., Chibazakura, T., Watanabe, S., and Yoshikawa, H. (2011). Interactions between histidine kinase NblS and the response regulators RpaB and SrrA are involved in the bleaching process of the cyanobacterium *Synechococcus elongatus* PCC 7942. Plant Cell Physiol. *52*, 2115–2122.

Kizawa, A., Kawahara, A., Takashima, K., Takimura, Y., Nishiyama, Y., and Hihara, Y. (2017). The LexA transcription factor regulates fatty acid biosynthetic genes in the cyanobacterium *Synechocystis* sp. PCC 6803. Plant J. Cell Mol. Biol. *92*, 189–198.

Kizawa, A., Kawahara, A., Takimura, Y., Nishiyama, Y., and Hihara, Y. (2016). RNA-seq profiling reveals novel target genes of LexA in the cyanobacterium *Synechocystis* sp. PCC 6803. Front. Microbiol. *7*. https://doi.org/10.3389/fmicb.2016.00193.

Köbler, C., Schultz, S.-J., Kopp, D., Voigt, K., and Wilde, A. (2018). The role of the *Synechocystis* sp. PCC 6803 homolog of the circadian clock output regulator RpaA in day-night transitions. Mol. Microbiol. *110*, 847–861.

Komenda, J., Barker, M., Kuviková, S., de Vries, R., Mullineaux, C.W., Tichý, M., and Nixon, P.J. (2006). The FtsH protease slr0228 is important for quality control of photosystem II in the thylakoid membrane of *Synechocystis* sp. PCC 6803. J. Biol. Chem. *281*, 1145–1151.

Kopf, M., and Hess, W.R. (2015). Regulatory RNAs in photosynthetic cyanobacteria. FEMS Microbiol. Rev. *39*, 301–315.

Kopf, M., Klähn, S., Scholz, I., Matthiessen, J.K.F., Hess, W.R., and Voß, B. (2014). Comparative analysis of the primary transcriptome of *Synechocystis* sp. PCC 6803. DNA Res. *21*, 527–539.

Krynická, V., Tichý, M., Krafl, J., Yu, J., Kaňa, R., Boehm, M., Nixon, P.J., and Komenda, J. (2014). Two essential FtsH proteases control the level of the Fur repressor during iron deficiency in the cyanobacterium *Synechocystis* sp. PCC 6803. Mol. Microbiol. *94*, 609–624.

Kunert, A., Vinnemeier, J., Erdmann, N., and Hagemann, M. (2003). Repression by Fur is not the main mechanism controlling the iron-inducible isiAB operon in the cyanobacterium *Synechocystis* sp. PCC 6803. FEMS Microbiol. Lett. *227*, 255–262.

Laudenbach, D.E., and Straus, N.A. (1988). Characterization of a cyanobacterial iron stress-induced gene similar to *psbC*. J. Bacteriol. *170*, 5018–5026.

Lawson, C.L., Swigon, D., Murakami, K.S., Darst, S.A., Berman, H.M., and Ebright, R.H. (2004). Catabolite activator protein: DNA binding and transcription activation. Curr. Opin. Struct. Biol. *14*, 10–20.

Lieman-Hurwitz, J., Haimovich, M., Shalev-Malul, G., Ishii, A., Hihara, Y., Gaathon, A., Lebendiker, M., and Kaplan, A. (2009). A cyanobacterial AbrB-like protein affects the apparent photosynthetic affinity for CO_2 by modulating low-CO_2-induced gene expression. Environ. Microbiol. *11*, 927–936.

Liu, L.-N., Bryan, S.J., Huang, F., Yu, J., Nixon, P.J., Rich, P.R., and Mullineaux, C.W. (2012). Control of electron transport routes through redox-regulated redistribution of respiratory complexes. Proc. Natl. Acad. Sci. U S A *109*, 11431–11436.

López-Redondo, M.L., Moronta, F., Salinas, P., Espinosa, J., Cantos, R., Dixon, R., Marina, A., and Contreras, A. (2010). Environmental control of phosphorylation pathways in a branched two-component system: NblS, a branched two-component system. Mol. Microbiol. *78*, 475–489.

Marin, K., Suzuki, I., Yamaguchi, K., Ribbeck, K., Yamamoto, H., Kanesaki, Y., Hagemann, M., and Murata, N. (2003). Identification of histidine kinases that act as sensors in the perception of salt stress in *Synechocystis* sp. PCC 6803. Proc. Natl. Acad. Sci. U S A *100*, 9061–9066.

Martin, W., Rujan, T., Richly, E., Hansen, A., Cornelsen, S., Lins, T., Leister, D., Stoebe, B., Hasegawa, M., and Penny, D. (2002). Evolutionary analysis of Arabidopsis, cyanobacterial, and chloroplast genomes reveals plastid phylogeny and thousands of cyanobacterial genes in the nucleus. Proc. Natl. Acad. Sci. U S A *99*, 12246–12251.

Mikami, K., Kanesaki, Y., Suzuki, I., and Murata, N. (2002). The histidine kinase Hik33 perceives osmotic stress and cold stress in *Synechocystis* sp. PCC 6803. Mol. Microbiol. *46*, 905–915.

Mitschke, J., Georg, J., Scholz, I., Sharma, C.M., Dienst, D., Bantscheff, J., Voß, B., Steglich, C., Wilde, A., Vogel, J., et al. (2011). An experimentally anchored map of transcriptional start sites in the model cyanobacterium *Synechocystis* sp. PCC6803. Proc. Natl. Acad. Sci. U S A *108*, 2124–2129.

Moronta-Barrios, F., Espinosa, J., and Contreras, A. (2012). In vivo features of signal transduction by the essential response regulator RpaB from *Synechococcus elongatus* PCC 7942. Microbiology *158*, 1229–1237.

Mullineaux, C.W. (2014). Electron transport and light-harvesting switches in cyanobacteria. Front. Plant Sci. *5*. https://doi.org/10.3389/fpls.2014.00007.

Munekage, Y., Hojo, M., Meurer, J., Endo, T., Tasaka, M., and Shikanai, T. (2002). PGR5 is involved in cyclic electron flow around photosystem I and is essential for photoprotection in Arabidopsis. Cell *110*, 361–371.

Murata, N., and Los, D.A. (2006). Histidine kinase Hik33 is an important participant in cold-signal transduction in cyanobacteria. Physiol. Plant *126*, 17–27.

Oliveira, P., and Lindblad, P. (2005). LexA, a transcription regulator binding in the promoter region of the bidirectional hydrogenase in the cyanobacterium Synechocystis sp. PCC 6803. FEMS Microbiol. Lett. *251*, 59–66.

Piechura, J.R., Amarnath, K., and O'Shea, E.K. (2017). Natural changes in light interact with circadian regulation at promoters to control gene expression in cyanobacteria. Elife *6*. https://doi.org/10.7554/eLife.32032.

Riediger, M., Hihara, Y., and Hess, W.R. (2018). From cyanobacteria and algae to land plants: the RpaB/Ycf27 regulatory network in transition. Perspect. Phycol. *5*, 13–25.

Sánchez-Riego, A.M., López-Maury, L., and Florencio, F.J. (2013). Glutaredoxins are essential for stress adaptation in the cyanobacterium Synechocystis sp. PCC 6803. Front. Plant Sci. *4*. https://doi.org/10.3389/fpls.2013.00428.

Saroussi, S.I., Wittkopp, T.M., and Grossman, A.R. (2016). The type II NADPH dehydrogenase facilitates cyclic electron flow, energy-dependent quenching, and chlororespiratory metabolism during acclimation of *Chlamydomonas reinhardtii* to nitrogen deprivation. Plant Physiol. *170*, 1975–1988.

Scholz, I., Lange, S.J., Hein, S., Hess, W.R., and Backofen, R. (2013). CRISPR-Cas systems in the cyanobacterium *Synechocystis* sp. PCC6803 exhibit distinct processing pathways involving at least two Cas6 and a Cmr2 protein. PLoS One *8*, e56470.

Seino, Y., Takahashi, T., and Hihara, Y. (2009). The response regulator RpaB binds to the upstream element of photosystem I genes to work for positive regulation under low-light conditions in *Synechocystis* sp. strain PCC 6803. J. Bacteriol. *191*, 1581–1586.

Seki, A., Hanaoka, M., Akimoto, Y., Masuda, S., Iwasaki, H., and Tanaka, K. (2007). Induction of a group 2 σ factor, RPOD3, by high light and the underlying mechanism in *Synechococcus elongatus* PCC 7942. J. Biol. Chem. *282*, 36887–36894.

Shikanai, T. (2014). Central role of cyclic electron transport around photosystem I in the regulation of photosynthesis. Curr. Opin. Biotechnol. *26*, 25–30.

Suzuki, I., Los, D.A., Kanesaki, Y., Mikami, K., and Murata, N. (2000). The pathway for perception and transduction of low-temperature signals in *Synechocystis*. EMBO J. *19*, 1327–1334.

Takahashi, T., Nakai, N., Muramatsu, M., and Hihara, Y. (2010). Role of multiple HLR1 sequences in the regulation of the dual promoters of the *psaAB* genes in *Synechocystis* sp. PCC 6803. J. Bacteriol. *192*, 4031–4036.

Tan, G., and Lenhard, B. (2016). TFBSTools: an R/bioconductor package for transcription factor binding site analysis. Bioinforma. Oxf. Engl. *32*, 1555–1556.

Tu, C.-J., Shrager, J., Burnap, R.L., Postier, B.L., and Grossman, A.R. (2004). Consequences of a deletion in *dspA* on transcript accumulation in *Synechocystis* sp. strain PCC6803. J. Bacteriol. *186*, 3889–3902.

van Waasbergen, L.G., Dolganov, N., and Grossman, A.R. (2002). *nblS*, a gene involved in controlling photosynthesis-related gene expression during high light and nutrient stress in *Synechococcus elongatus* PCC 7942. J. Bacteriol. *184*, 2481–2490.

Vinnemeier, J., Kunert, A., and Hagemann, M. (1998). Transcriptional analysis of the *isiAB* operon in salt-stressed cells of the cyanobacterium *Synechocystis* sp. PCC 6803. FEMS Microbiol. Lett. *169*, 323–330.

Wilde, A., and Hihara, Y. (2016). Transcriptional and posttranscriptional regulation of cyanobacterial photosynthesis. Biochim. Biophys. Acta *1857*, 296–308.

Yeremenko, N., Jeanjean, R., Prommeenate, P., Krasikov, V., Nixon, P.J., Vermaas, W.F.J., Havaux, M., and Matthijs, H.C.P. (2005). Open reading frame *ssr2016* is required for antimycin A-sensitive photosystem I-driven cyclic electron flow in the cyanobacterium *Synechocystis* sp. PCC 6803. Plant Cell Physiol. *46*, 1433–1436.

Yeremenko, N., Kouril, R., Ihalainen, J.A., D'Haene, S., van Oosterwijk, N., Andrizhiyevskaya, E.G., Keegstra, W., Dekker, H.L., Hagemann, M., Boekema, E.J., et al. (2004). Supramolecular organization and dual function of the IsiA chlorophyll-binding protein in cyanobacteria. Biochemistry *43*, 10308–10313.

Zer, H., Margulis, K., Georg, J., Shotland, Y., Kostova, G., Sultan, L.D., Hess, W.R., and Keren, N. (2018). Resequencing of a mutant bearing an iron starvation recovery phenotype defines Slr1658 as a new player in the regulatory network of a model cyanobacterium. Plant J. *93*, 235–245.

Zhang, P., Sicora, C.I., Vorontsova, N., Allahverdiyeva, Y., Battchikova, N., Nixon, P.J., and Aro, E.-M. (2007). FtsH protease is required for induction of inorganic carbon acquisition complexes in *Synechocystis* sp. PCC 6803. Mol. Microbiol. *65*, 728–740.

ISCI, Volume *15*

Supplemental Information

Biocomputational Analyses and Experimental Validation

Identify the Regulon Controlled

by the Redox-Responsive Transcription Factor RpaB

Matthias Riediger, Taro Kadowaki, Ryuta Nagayama, Jens Georg, Yukako Hihara, and Wolfgang R. Hess

Supplemental Information

TRANSPARENT METHODS

Bioinformatics Methods

A workflow illustrating the major bioinformatics steps, tools, important data and results is given in **Figure 1.** A *Synechocystis* 6803 promoter database was set up and the HLR1 motif defined as presented in **Figure 1.** Motifs were detected with the Bioconductor package TFBSTools (Tan and Lenhard, 2016) with a relative motif score ≥ 0.9, and integrated with previously obtained differential RNA-Seq data (Kopf et al., 2014) providing precise information on transcriptional start sites (TSSs). The average relative expression of all promoters with an HLR1 at the same relative position was plotted against the motif's distance to the TSS and further examined as outlined in **Figure 1.**

Strains and growth conditions

Synechocystis 6803 was grown in BG11 (Stanier et al., 1971) buffered with 20 mM N-[Tris(hydroxymethyl)methyl]-2-aminoethanesulfonic acid (TES), pH 7.6, at 30°C at 50 µmol quanta $*$ m^{-2} $*$ s^{-1} of white light under slight agitation ± selective antibiotics (kanamycin, Km: 50 µg$*$$mL^{-1}$, chloramphenicol, Cm: 20 mg$*$$mL^{-1}$). To induce HL stress, cultures were shifted from 30 to 300 µmol quanta $*$ m^{-2} $*$ s^{-1}. To induce iron deficiency, 300 µM desferrioxamin B (DFB) was added to liquid cultures. To induce nitrogen deficiency, cells were centrifuged, washed and cultivated in NO_3^--free BG11.

Construction, expression and purification of *E. coli* strains expressing His-tagged transcription factors

The coding region of *furA* (*sll0567*) was amplified by PCR using the primers *Nde*I-FurA-fw and *Xho*I-FurA-rv (oligonucleotides are listed in **Table S4**) and cloned into the pT7Blue T-vector (Novagen). The *furA* PCR fragments were excised from the pT7Blue vector with *Nde*I and *Xho*I and subcloned into the same restriction sites in vector pET28a r (Novagen) to express proteins with an N-terminal 6xHis-tag. Following transformation into *E. coli* ArcticExpress (DE3)RIL competent cells (Agilent), the strains harboring the Fur expression construct were precultured in 5 mL LB medium containing 50 $\mu g{*}mL^{-1}$ kanamycin at 37°C overnight. The preculture was seeded into 500 mL LB and FurA expression was induced with 100 µM IPTG from midlog cultures grown overnight at 15°C. Purification of His-Fur proteins was performed on a nickel column using the ÄKTA start system (GE Healthcare). The purity of His-FurA was checked by SDS-PAGE. The preparation was desalted by PD MidiTrap G-25 (GE Healthcare) and concentrations were determined via Bradford assay. The construction, expression and purification of *E. coli* strains expressing His-tagged RpaB was performed as described (Kadowaki et al., 2016).

Chromatin Affinity Purification (ChAP)

Preparation of whole-cell extracts for ChAP analysis, affinity purification of His-RpaB and DNA were performed as described (Kadowaki et al., 2016) with some modifications as follows. A 0.5 mg aliquot of protein of the whole-cell extract and 10 µL of Dynabeads His-Tag Isolation and Pulldown (Veritas) were used for affinity purification of His-RpaB, followed by further purification steps and quantitative real-time PCR analysis as described (Kadowaki et al., 2016).

Northern blot

Isolation of RNA by the hot-phenol method and RNA gel blot analyses using the DIG RNA labeling and detection kit (Roche) were performed as described (Kadowaki et al., 2016). To facilitate the direct use of PCR products as templates for *in vitro* transcription, the T7 polymerase promoter (TAATACGACTCACTATAGGGCGA) was added at the 5' termini of the reverse primers.

Electrophoretic mobility shift assay (EMSA)

The *nirA* and *ftsH2* promoter fragments, with or without mutations, were PCR-amplified from *Synechocystis* genomic DNA using Go Taq Hot Start Green Master Mix. Native and mutated promoter regions of *pgr5*, *gcvP*, *psrR1* and *lexA* were generated by annealing overlapping primers and filling up without template DNA. Native and mutated versions of the *isiA* promoter were amplified from the pILA vector containing this promoter (Kunert et al., 2000). The DNA fragments were 3' end-labeled with digoxigenin (DIG)-ddUTP by terminal transferase according to the manufacturer's instructions (DIG gel shift kit; Roche) with some modifications to remove EDTA using NucleoSpin Gel and PCR Clean-up (Macherey-Nagel). Assays were performed as described (Georg et al., 2017; Kadowaki et al., 2016).

Luciferase assay

Promoters containing predicted motifs of interest were amplified, encompassing ~400 nt upstream of the TSS, and introducing *Age*I and *Fse*I restriction sites at the 5' and 3' ends, respectively. PCR products were double-digested, ligated with the linearized empty pILA vector and transformed into chemically competent *E. coli* DH5α cells. To introduce site-directed mutagenesis, non-overlapping primers containing the desired mutation were designed by using the NEBaseChanger web tool (http://nebasechanger.neb.com/), followed by inverse PCR. The generated amplicons were *Dpn*I digested, phosphorylated, self-ligated and transformed into chemically competent *E. coli* DH5α cells. Following DNA preparation and cleavage by *Age*I and *Fse*I, the promoters of interest were inserted upstream of the *luxAB* 5'UTR in plasmid pILA (Kunert et al., 2000). The *Synechocystis* 6803 luciferase reporter strains harbored the decanal-producing plasmid pTCmYfr2luxCDE containing a *luxCDE* cassette with the Cm marker under control of the *yfr2a* promoter (Klähn et al., 2014; Voss et al., 2009). A strain harboring only the decanal-producing plasmid served as a negative control. Liquid precultures (two biological replicates per strain) were diluted (OD_{750} = 0.1) prior to analysis and cultivated to exponential phase (OD_{750} = 0.6 – 0.8). Prior to measurement, cells were diluted to an OD_{750} = 0.6, aliquots of 100 µL were transferred in three technical replicates per strain to a 96-well microtiter plate (PerkinElmer) and luminescence was measured as reported (Klähn et al., 2014).

Statistical Analysis

All bioinformatics related works were statistically analyzed using R. The cutoff for motif search using TFBSTools (Tan and Lenhard, 2016) was set to a relative motif score ≥ 0.9. The enriched areas were defined by a density threshold ≥ 99%. In addition, a probability of ≥ 0.95 had to be met for each promoter within these areas. For the functional enrichment using DAVID (Huang et al., 2009a, 2009c, 2009b) an enrichment score ≥ 1 was selected. Experimental data are presented as the mean ± standard deviation (SD). A two-tailed unpaired Student's t test was conducted for ChAP analysis to check for significance.

Data and Software Availability

All code involving the bioinformatics workflow including the input datasets is available on Github (https://github.com/MatthiasRiediger/Biocomputational-analyses-to-identify-the-regulon-controlled-by-RpaB.git)

SUPPLEMENTAL FIGURES

	1	2	3	4	5	6	7	8	9	10	11	12	13	14	15	16	17	18
A	-1.52	-2.49	-0.46	1.82	-1.71	1.73	0.90	0.45	0.73	0.20	-2.49	-4.29	0.15	1.78	-1.52	1.69	0.66	0.84
C	-4.16	-6.81	-2.03	-4.16	1.77	-1.78	-2.34	-3.28	-0.80	0.41	-6.81	-6.81	-2.03	-2.73	1.64	-2.03	-2.03	-1.78
G	0.86	-4.15	-2.33	-2.72	-2.33	-2.33	-1.76	-3.26	-1.55	-0.38	-0.29	-4.15	-2.72	-3.26	-4.15	-2.72	-1.36	-3.26
T	0.82	1.81	1.40	-3.44	-1.95	-4.30	0.56	1.15	0.38	-0.39	1.51	1.87	1.21	-2.90	-0.75	-2.20	0.71	0.71

Figure S1 Position specific weight matrix (PSWM) of HLR1 (related to **Figure 1 and 2**). HLR1 from 90 previously described motifs found in 83 promoters in *Synechocystis* 6803, *S. elongatus*, other cyanobacteria and eukaryotic algae (Riediger et al., 2018) was used as input for the global motif search .

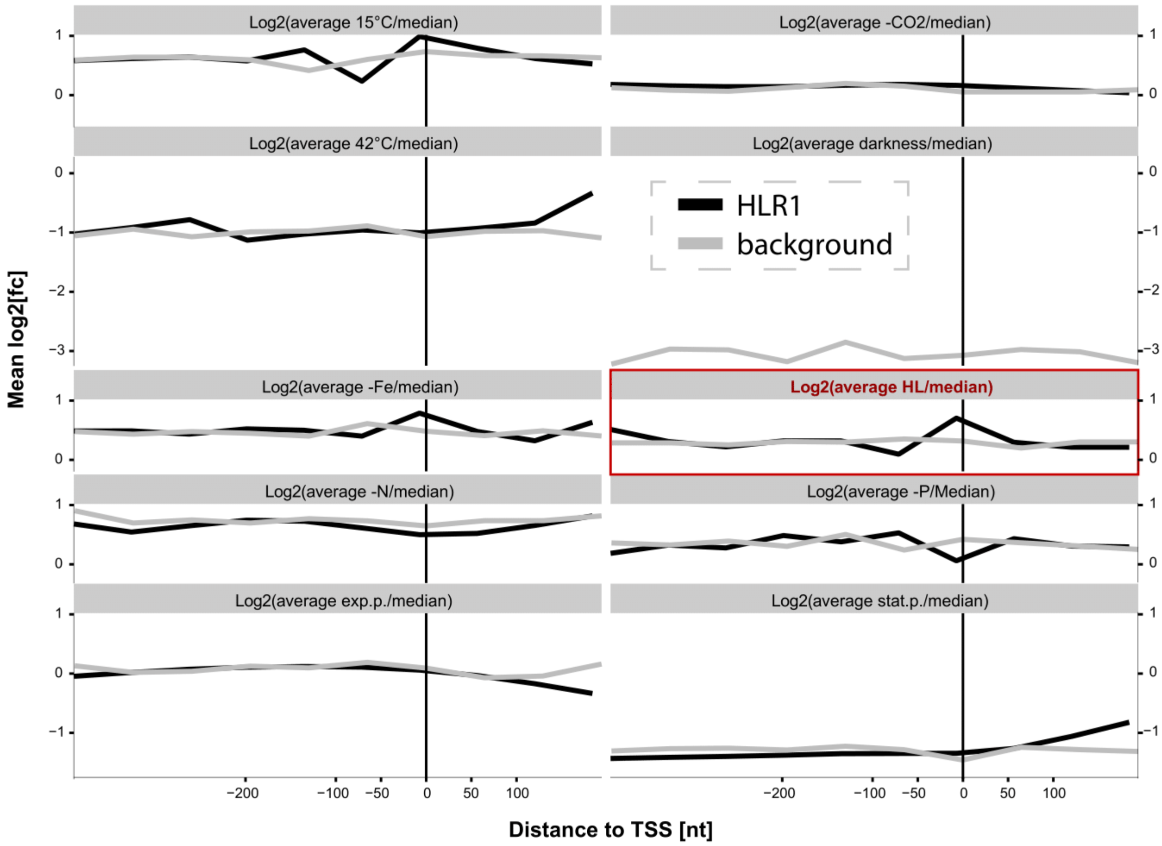

Figure S2 Positional dependency of HLR1 to relative expression under various conditions (related to **Figure 1 and 2**). Average relative expression (genewise: condition / median expression) of all genes having an HLR1 at the same relative position within their promoters plotted against the distance of the motif to the TSS. The data were taken from the ten different conditions investigated by differential RNA-Seq (Kopf et al., 2014). The same analysis was performed with the background model as a negative control.

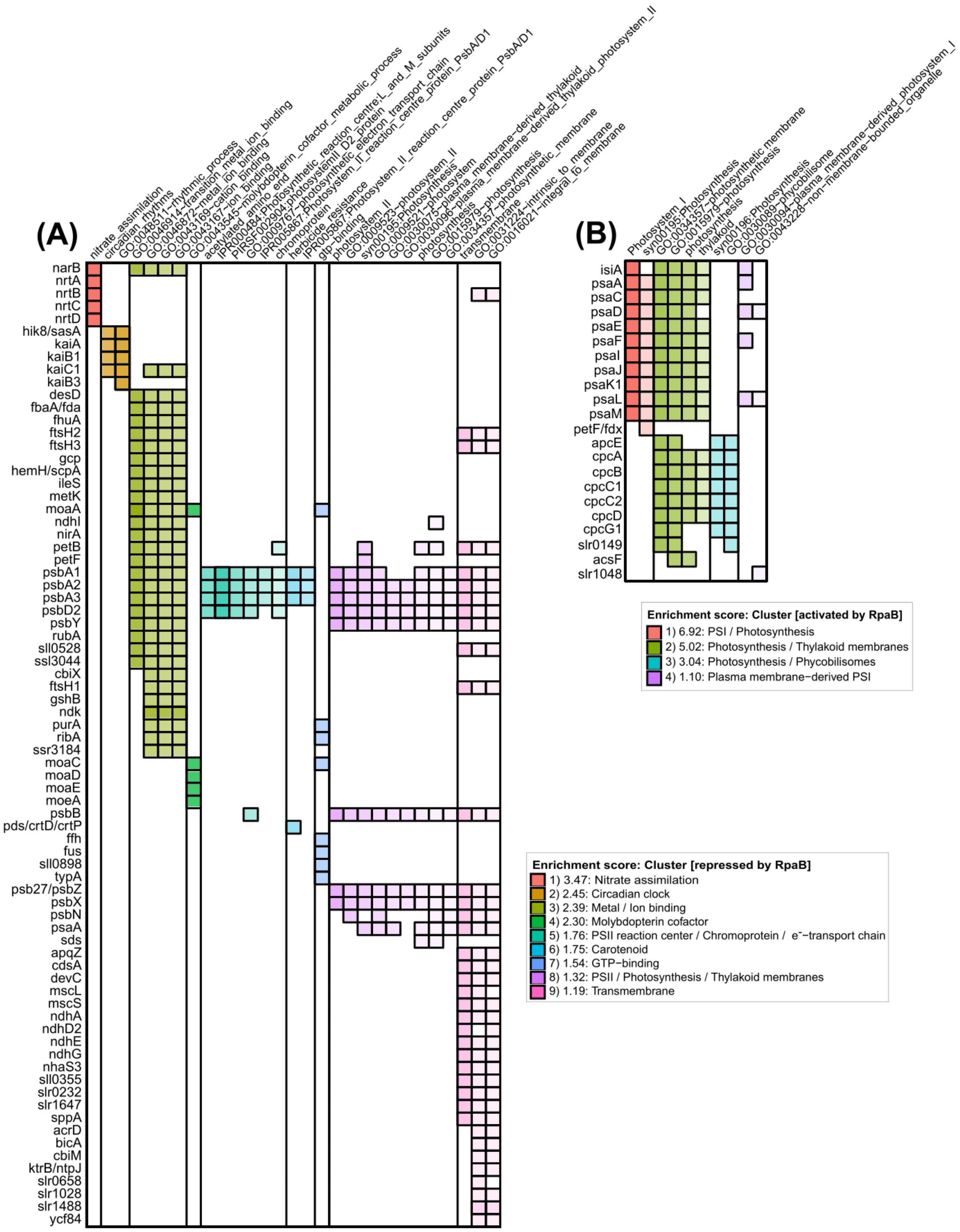

Figure S3 Functional enrichment analysis (related to **Figure 1 and 3**). Gene clusters which were predicted to be regulated by RpaB are shown in a heat map. **(A)** repressed, **(B)** activated genes. A probability threshold ≥75% was set to perform the functional enrichment analysis by using DAVID 6.7 (Huang et al., 2009a, 2009c, 2009b). All clusters with a highly stringent enrichment score ≥ 1 are shown (see also **Table S2** for further information).

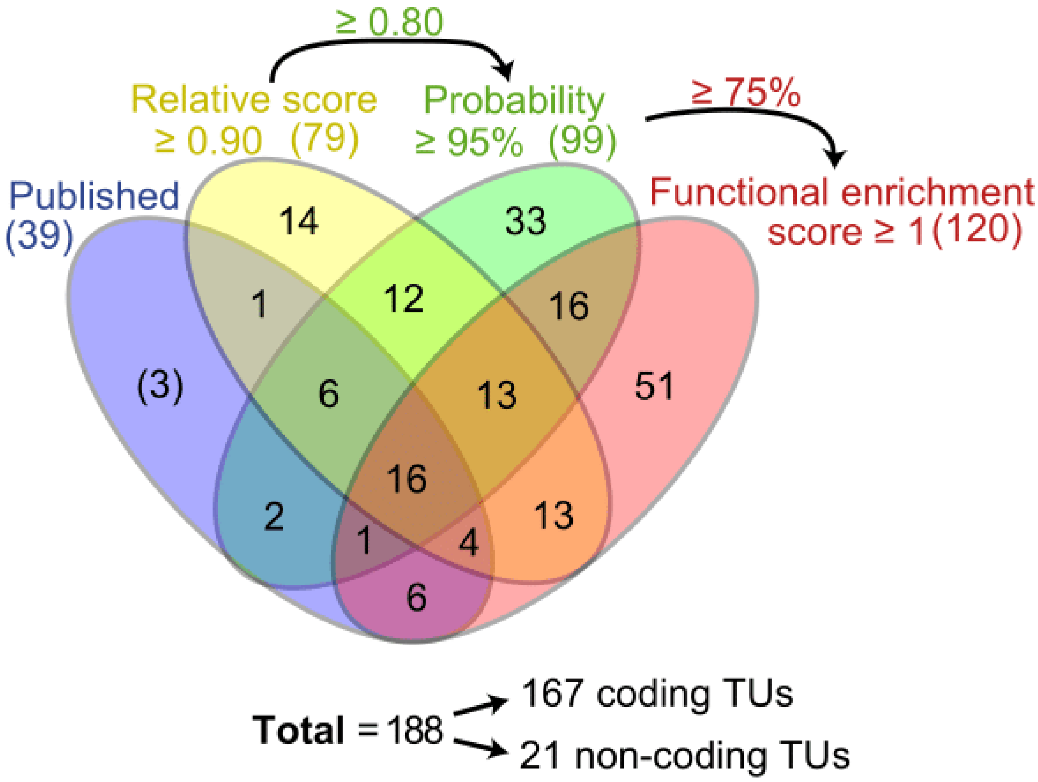

Figure S4 Number of mutually and individually detected target genes via different approaches (related to **Figure 3**). Venn diagram showing the number of genes or operons detected here by the combination of the three given parameters compared to the number of previously published targets in *Synechocystis* 6803. The selected parameters for the further analyses (motif score ≥ 0.80, probability ≥ 75%) and for the acceptance for the final regulon (motif score ≥ 0.90, probability ≥ 95%, functional enrichment score ≥ 1) as well as the total number of coding and non-coding TUs of the final regulon with these parameter settings are given.

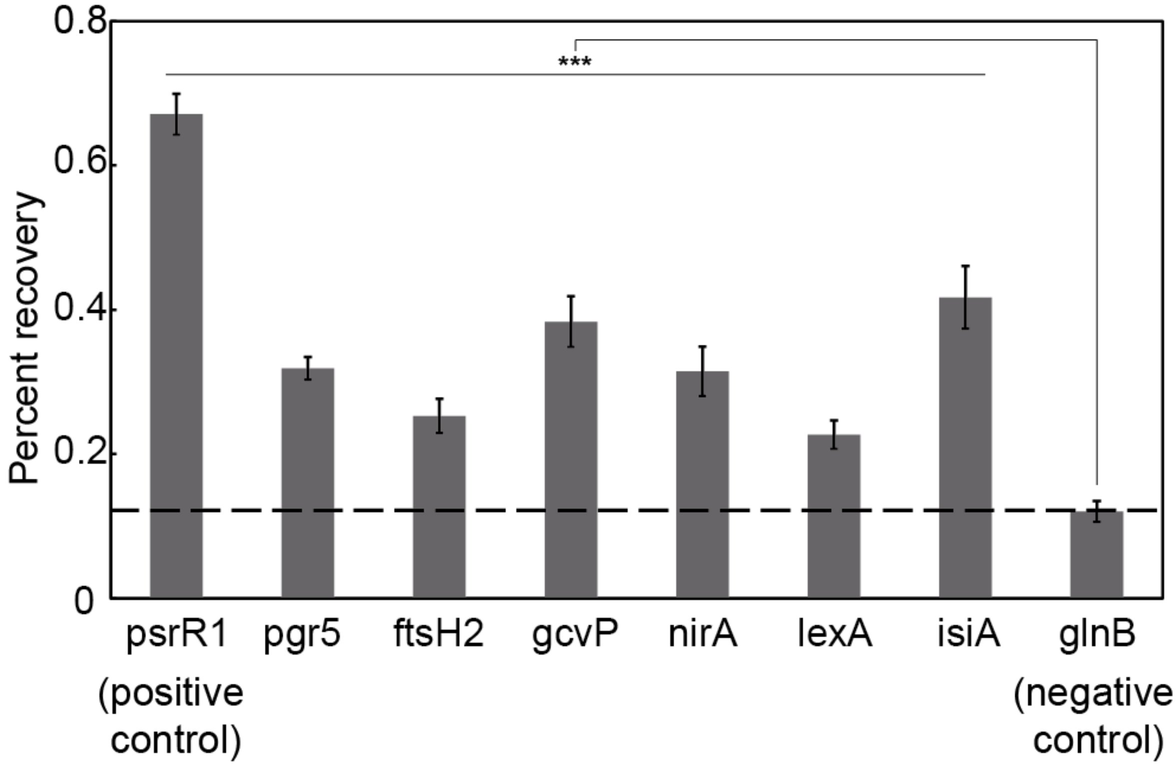

Figure S5 Binding activity of RpaB to the putative target promoters under LL conditions examined by ChAP (related to **Figure 5 and 6**). The level of DNA co-purified by nickel chromatography was determined by qPCR analysis and is given as percentage recovery relative to the total input DNA (negative control: *glnB*). Data represent means ± SD from three independent experiments. Statistical analysis was performed using two-tailed unpaired Student’s t test (*** $p < 0.001$).

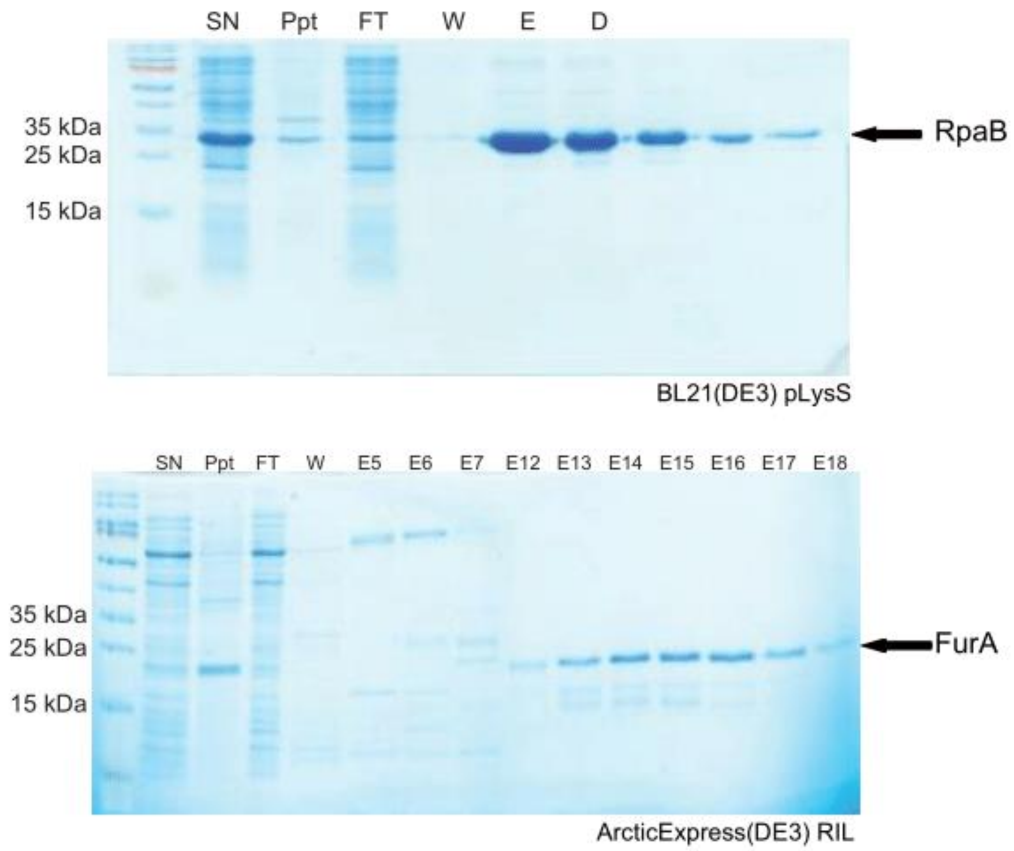

Figre S6 Coomassie gel showing the purification of His-RpaB and His-FurA by nickel affinity chromatography (related to **Figure 5 and 6**). The soluble fraction from an *E. coli* over-expression strain was loaded onto a HiTrap chelating HP column (GE Healthcare). Aliquots of supernatant (SN), insoluble precipitation (Ppt), flow-through (FT), wash (W) and eluate (E) fractions were separated by SDS-PAGE and stained with Coomassie Brilliant Blue.

Supplemental Tables

Supplemental **Tables S1 to S3** are provided as separate Excel files.

Table S4 Desoxyoligonucleotide sequences (related to **Figure 5** and **Figure 6**).

Name	**Sequence** (lowercase letters indicate mutated sites)	**Purpose**
NdeI-FurA-F	AACATATGTCCTACACCGCCGAT	Construction of His-Fur
XhoI-FurA-R	AACTCGAGCTAGGCCAAGGAAATACT	Construction of His-Fur
qRT-psrR1-F	CCCTCAACTTTGTCCGCATTG	ChAP
qRT-psrR1-R	TTCTGTCGGGTTTCCATAGCC	ChAP
qRT-pgr5-F	CAAACCGCATCTAACGCCAAG	ChAP
qRT-pgr5-R	GGGGGAAACTTTCTTTGCCTTATG	ChAP
qRT-ftsH2-F	GGTGAATATTTTGCGGTGATCCTC	ChAP
qRT-ftsH2-R	GACGCCGTGGAATTGATTAATTTTGTTGAC	ChAP
qRT-gcvP-F	TTGGCAATGCTGACCCCTAG	ChAP
qRT-gcvP-R	AAGGATGAACGCCTGGACTG	ChAP
qRT-nirA-F	CGTAAACTGCATATGCCTTGGC	ChAP
qRT-nirA-R	ACGCTTCAAGCCAGATAACAGTAG	ChAP
qRT-lexA-F	TGGCCGAAAATGAGGAACCG	ChAP
qRT-lexA-R	GGACTCTAGGACTATTTTAAACCCAGTC	ChAP
qRT-isiA-F	AAATCCTCACCTGGCCATGG	ChAP
qRT-isiA-R	AGCACTTACTCCCGAATTATTATAGGG	ChAP
qRT-glnB-F	CAAGGGTTCACCAAATCCAG	ChAP
qRT-glnB-R	CTCGTGCAATGATCTGGTTG	ChAP
pgr5-F	ATGTTCGCCCCCATCGTTA	Northern blot
T7-pgr5-R	TAATACGACTCACTATAGGGCGATTAGGCCAATAAACCGAGGGT	Northern blot
ftsH2-F	CAAAGAGAATGCCCCCTGTTTG	Northern blot
T7-ftsH2-R	TAATACGACTCACTATAGGGCGAGTCCACGGCATCATCAATTTCC	Northern blot
gcvP-F	GTTTGGCATTCCCTTGGGTTAC	Northern blot
T7-gcvP-R	TAATACGACTCACTATAGGGCGATTCCGCCGCTTTCAAAATGG	Northern blot
nirA-F	TCGAAGGAAGCCGGGATAATTC	Northern blot
T7-nirA-R	TAATACGACTCACTATAGGGCGACCACGTAATTTAACCCGGCTTG	Northern blot
lexA-F	GGCCATGAATTTGCGTTCTCC	Northern blot
T7-lexA-R	TAATACGACTCACTATAGGGCGAACGACCTTAGTGCCATCTTGG	Northern blot
isiA-F	CGATGGCGGACAAATTGTGG	Northern blot
T7-isiA-R	TAATACGACTCACTATAGGGCGAATGGCTTCCCCGGAAAAGAG	Northern blot
Ppgr5 (fw)	CTTGTCAACTTTGCTTTACAAAAATTTACAAAACTGTTACATTTATTTACATAAG	electrophoretic mobility shift assay
Ppgr5 (rv)	CTTATGGGGGAAACTTTCTTTGCCTTATGTAAATAAATGTAACAGTTTTG	electrophoretic mobility shift assay
Ppgr5 HLR1a sub (fw)	CTTGTCAACTTTGCccccCAAAAATccccAAAACTGTTACATTTATTTACATAAG	electrophoretic mobility shift assay, site directed mutagenesis
Ppgr5 HLR1b sub (fw)	CTTGTCAACTTTGCTTTACAAAAATTTACAAAACTccccCATTTATccccATAAG	electrophoretic mobility shift assay, site directed mutagenesis
Ppgr5 HLR1b sub (rv)	CTTATGGGGGAAACTTTCTTTGCCTTATggggATAAATggggG	electrophoretic mobility shift assay, site directed mutagenesis
Ppgr5 HLR1a+b sub (fw)	CTTGTCAACTTTGCccccCAAAAATccccAAAACTccccCATTTATccccATAAG	electrophoretic mobility shift assay, site directed mutagenesis

PftsH2 (fw)	GAGAATTACGTTACATTTAGTTAAGATTTTGTTACAAAACTCCG	electrophoretic mobility shift assay
PftsH2 (rv)	GCTCCCCGACGCCGTGGAATTGATTAATTTTGTTGACAACGGAGTTTTGTAACAAAATC	electrophoretic mobility shift assay
PftsH2 HLR1 sub (fw)	GAGAATTACccccCATTTAGccccGATTTTGTTACAAAACTCCG	electrophoretic mobility shift assay, site directed mutagenesis
PlexA (fw)	CGGCGATCGCCTTCTGCTGGCCGAAAATGAGGAACCGTCGGAAGA	electrophoretic mobility shift assay
PlexA (rv)	CATACTAAAAAAGATACAAAATTTTACATTTCTTCCGACGGTTCCTC	electrophoretic mobility shift assay
PgcvP (fw)	CTACCAAAATTTGTTAAGCTTTGTATCTAATTAGAGCCAATCT	electrophoretic mobility shift assay
PgcvP (rv)	CGCCTGGACTGGATCTGTCAAAAAATGTTACAGATTGGCTCTAATTAGAT	electrophoretic mobility shift assay
PgcvP HLR1a sub (fw)	CTACCAAAAccccTTAAGCTccccATCTAATTAGAGCCAATCT	electrophoretic mobility shift assay, site directed mutagenesis
PgcvPHLR1b sub (rv)	CGCCTGGACTGGATCTggggAAAAATGggggAGATTGGCTCTAATTAGAT	electrophoretic mobility shift assay, site directed mutagenesis
nirA (fw)	GAGTGTAATTTACGTTACAAATTTTAACGAAACGGGAACCCTATATTG	electrophoretic mobility shift assay
nirA (rv)	AACGCTTCAAGCCAGATAACAGTAGAGATCAATATAGGGTTCCCGTTTC	electrophoretic mobility shift assay
nirA HLR1 sub (fw)	GAGTGTAATTTACccccCAAATTTccccGAAACGGGAACCCTATATTG	electrophoretic mobility shift assay, site directed mutagenesis
PisiA (fw)	CCATGGGTTCAACCCTGC	electrophoretic mobility shift assay
PisiA (rv)	CTCCCGAATTATTATAGGGGC	electrophoretic mobility shift assay
isiA Fur1 sub (fw)	GTTGCTATAAATccccccTTATGCCCCTATAATAATTCGGG	electrophoretic mobility shift assay, site directed mutagenesis
isiA HLR1 sub (fw)	TAAAATTggggAGAAATGggggGCAGGGTTGAACCCATGG	electrophoretic mobility shift assay, site directed mutagenesis
isiA (rv)	TAAAATTATTAAGAAATGTTAAGCAGGGTTGAACCCATGG	electrophoretic mobility shift assay, site directed mutagenesis
isiA (fw)	GTTGCTATAAATTCTCATTTATGCCCCTATAATAATTCGGG	electrophoretic mobility shift assay, site directed mutagenesis
PpsrR (fw)	GTGGGACACGCACCACTA	electrophoretic mobility shift assay
PpsrR1 (rv)	GTTTCCATAGCCTTATGT	electrophoretic mobility shift assay
PpsrR1 sub1 (rv)	GTTTCCATAGCCTTATGTTTTTTATAGTAAACATAATgggg	electrophoretic mobility shift assay, site directed mutagenesis
luxA seq (rv)	CAAGCCGAACAAAGCGATCC	sequencing primer pILA
pILA seq (fw)	CGCATAGAAATTGCATCAACGC	sequencing primer pILA
pIGA (fw)	CTCAGCGCCAAGAGTAGTTCC	segregation primer pILA
pIGA (rv)	CACTCTGCACTGTGTCTGTGC	segregation primer pILA
pJet seq (fw)	ATCTTACTACTCGATGAGTTTTCG	sequencing primer pJET
pJet seq (rv)	AGAGTCGATTGCCAAGAAAACC	sequencing primer pJET
PftsH2 ageI (fw)	TTACCGGTGACCCATGGCAGTGTCC	luciferase assay
PftsH2 fseI (rv)	AAAGGCCGGCCATGTTAGCTCACTTTAAAAGTTAAGAC	luciferase assay
PgcvP ageI (fw)	TTACCGGTTGGACGAGTTTTATGGGG	luciferase assay
PgcvP fseI (rv)	AAAGGCCGGCCAATGGCGGAGTAGGGAA	luciferase assay
PlexA fseI (rv)	AAAGGCCGGCCGTAATATCTCCTATAGGAATGTATTTAGG	luciferase assay
PlexA ageI (fw)	TTACCGGTTTTCGCCCTCAATCACAG	luciferase assay
PnirA ageI (fw)	TTACCGGTTCAGAATGCTGCGGGGA	luciferase assay
PnirA fseI (rv)	AAAGGCCGGCCAACGCTTCAAGCCAGATAACAG	luciferase assay
Ppgr5 ageI (fw)	TTACCGGTCGGACAATTGATCAAGCCA	luciferase assay
Ppgr5 fseI (rv)	AAAGGCCGGCCGGCAGTGACTCCTAAATTCC	luciferase assay
PftsH2 HLR1 mut (fw)	TAGccccGATTTTGTTACAAAACTCCGTTG	luciferase assay, site directed mutagenesis
PftsH2 HLR1 mut (rv)	AATGTAACGTAATTCTCATAATTACGA	luciferase assay, site directed mutagenesis
PgcvP HLR1a mut (fw)	CTccccATCTAATTAGAGCCAATCTGTAAC	luciferase assay, site directed mutagenesis
PgcvP HLR1a mut (rv)	CTTAACAAATTTTGGTAGGCCT	luciferase assay, site directed mutagenesis
PisiA HLR1+Fur mut (fw)	TTccccCTATAAATTCTCATTTATGCCC	luciferase assay, site directed mutagenesis
PisiA HLR1+Fur mut (rv)	AATTccccAGAAATGTTAAGCAGGGTTG	luciferase assay, site directed mutagenesis
PisiA Fur mut (fw)	=IsiA HLR1Fur mut (fw)	luciferase assay, site directed mutagenesis
PisiA Fur mut (rv)	AATTATTAAGAAATGTTAAGCAGG	luciferase assay, site directed mutagenesis
PisiA HLR1 mut (fw)	TTAGTTGCTATAAATTCTCATTTATG	luciferase assay, site directed mutagenesis

PisiA HLR1 mut (rv)	=IsiA HLR1Fur mut (rv)	luciferase assay, site directed mutagenesis
PlexA HLR1 mut (fw)	GTAAAATTccccATCTTTTTTAGTATGATTGCCCTG	luciferase assay, site directed mutagenesis
PlexA HLR1 mut (rv)	ATTTCTTCCGACGGTTCCTCATTTTCGGCCAG	luciferase assay, site directed mutagenesis
PnirA HLR1 mut (fw)	TggggCGAAACGGGAACCCTATATTGAT	luciferase assay, site directed mutagenesis
PnirA HLR1 mut (rv)	ATTTGTAACGTAAATTACACTCAGC	luciferase assay, site directed mutagenesis
PnirA HLR1+NtcA mut (fw)	ACAAATTggggCGAAACGGGAACCCTATATTG	luciferase assay, site directed mutagenesis
PnirA HLR1+NtcA mut (rv)	AACGTAAATgggACTCAGCCAAGGCATATG	luciferase assay, site directed mutagenesis
PnirA NtcA mut (fw)	ACGTTACAAATTTTAACGAAACGG	luciferase assay, site directed mutagenesis
PnirA NtcA mut (rv)	AAATgggACTCAGCCAAGGCATATG	luciferase assay, site directed mutagenesis
Ppgr5 HLR1a+b mut (fw)	CATTTATTTggggAAGGCAAAGAAAGTTTCC	luciferase assay, site directed mutagenesis
Ppgr5 HLR1a+b mut (rv)	TAACAGTTTccccAATTTTTGTAAAGCAAAGTTGAC	luciferase assay, site directed mutagenesis
Ppgr5 HLR1a mut (fw)	gggAAACTGTTACATTTATTTACATAAGG	luciferase assay, site directed mutagenesis
Ppgr5 HLR1a mut (rv)	cAATTTTTGTAAAGCAAAGTTGAC	luciferase assay, site directed mutagenesis
Ppgr5 HLR1b mut (fw)	gggAAGGCAAAGAAAGTTTCCC	luciferase assay, site directed mutagenesis
Ppgr5 HLR1b mut (rv)	cAAATAAATGTAACAGTTTTGTAAATTTTTG	luciferase assay, site directed mutagenesis

Supplemental references

Georg, J., Kostova, G., Vuorijoki, L., Schön, V., Kadowaki, T., Huokko, T., Baumgartner, D., Müller, M., Klähn, S., Allahverdiyeva, Y., et al. (2017). Acclimation of oxygenic photosynthesis to iron starvation is controlled by the sRNA IsaR1. Curr. Biol. *27*, 1425-1436.e7. https://doi.org/10.1016/j.cub.2017.04.010

Huang, D.W., Sherman, B.T., and Lempicki, R.A. (2009a). Bioinformatics enrichment tools: paths toward the comprehensive functional analysis of large gene lists. Nucleic Acids Res. *37*, 1–13. https://doi.org/10.1093/nar/gkn923

Huang, D.W., Sherman, B.T., and Lempicki, R.A. (2009b). Systematic and integrative analysis of large gene lists using DAVID bioinformatics resources. Nat. Protoc. *4*, 44–57. https://doi.org/10.1038/nprot.2008.211

Huang, D.W., Sherman, B.T., Zheng, X., Yang, J., Imamichi, T., Stephens, R., and Lempicki, R.A. (2009c). Extracting biological meaning from large gene lists with DAVID. Curr. Protoc. Bioinforma. Chapter *13*, Unit 13.11. https://doi.org/10.1002/0471250953.bi1311s27

Kadowaki, T., Nagayama, R., Georg, J., Nishiyama, Y., Wilde, A., Hess, W.R., and Hihara, Y. (2016). A feed-forward loop consisting of the response regulator RpaB and the small RNA PsrR1 controls light acclimation of photosystem I gene expression in the cyanobacterium *Synechocystis* sp. PCC 6803. Plant Cell Physiol. *57*, 813–823. https://doi.org/10.1093/pcp/pcw028

Klähn, S., Baumgartner, D., Pfreundt, U., Voigt, K., Schön, V., Steglich, C., and Hess, W.R. (2014). Alkane biosynthesis genes in cyanobacteria and their transcriptional organization. Front. Bioeng. Biotechnol. *2*. https://doi.org/10.3389/fbioe.2014.00024

Kopf, M., Klähn, S., Scholz, I., Matthiessen, J.K.F., Hess, W.R., and Voß, B. (2014). Comparative analysis of the primary transcriptome of *Synechocystis* sp. PCC 6803. DNA Res. *21*, 527–539. https://doi.org/10.1093/dnares/dsu018

Kunert, A., Hagemann, M., and Erdmann, N. (2000). Construction of promoter probe vectors for *Synechocystis* sp. PCC 6803 using the light-emitting reporter systems Gfp and LuxAB. J. Microbiol. Methods *41*, 185–194.

Riediger, M., Hihara, Y., and Hess, W.R. (2018). From cyanobacteria and algae to land plants: The RpaB/Ycf27 regulatory network in transition. Perspect. Phycol. *5*, 13–25. https://doi.org/10.1127/pip/2018/0078

Stanier, R.Y., Kunisawa, R., Mandel, M., and Cohen-Bazire, G. (1971). Purification and properties of unicellular blue-green algae (order Chroococcales). Bacteriol. Rev. *35*, 171–205.

Tan, G.; and Lenhard, B. (2016). TFBSTools: an R/bioconductor package for transcription factor binding site analysis. Bioinforma. Oxf. Engl. *32*, 1555–1556. https://doi.org/10.1093/bioinformatics/btw024

Voss, B., Georg, J., Schön, V., Ude, S., and Hess, W.R. (2009). Biocomputational prediction of non-coding RNAs in model cyanobacteria. BMC Genomics *10*, 123. https://doi.org/10.1186/1471-2164-10-123